Dissertation presented to the Instituto Tecnológico de Aeronáutica, in partial fulfilment of the requirements for the Degree of Master of Science in the Program of Aeronautics and Mechanical Engineering, Mechanics of Solids and Structures Area.

André Luiz Rocha D' Oliveira

NON-CONVENTIONAL METHOD PROPOSAL FOR RESIDUAL STRESS SIMULATION GENERATED BY END MILLING PROCESS

Dissertation approved in its final version by the signatories below:

Prof. Dr. Alfredo Rocha de Faria
Advisor

Prof. Dr. Luiz Carlos Sandoval Góes
Prorector of Graduate Studies and Research

Campo Montenegro
São José dos Campos, SP – Brazil
2016

BIBLIOGRAPHIC REFERENCE

OLIVEIRA, André Luiz Rocha D'. **Non-conventional method proposal for residual stress simulation generated by end milling process**. 2016. 99f. Dissertation of Master of Science in Mechanics of Solids and Structures – Instituto Tecnológico de Aeronáutica, São José dos Campos.

CESSION OF RIGHTS

NON CONVENTIONAL METHOD PROPOSAL FOR RESIDUAL STRESS SIMULATION GENERATED BY END MILLING PROCESS

André Luiz Rocha D' Oliveira

Thesis Committee Composition:

Prof. Dr.	Eliseu Lucena Neto	Chairperson	-	ITA
Prof. Dr.	Alfredo Rocha de Faria	Advisor	-	ITA
Prof. Dr.	Jefferson de Oliveira Gomes		-	ITA
Prof.ª Dr.ª	Eliene Oliveira Lucas		-	UFV, Viçosa

ITA

Dedico este trabalho à origem de todos meus princípios: meus avós, meus pais e meu irmão.

Agradecimentos

A lista de pessoas a quem eu devo agradecer é tão grande que mais de uma dissertação seria necessária para expressá-la. Tentarei ser o mais direto possível, ficando meu muito obrigado desde já para todas as pessoas que direta ou indiretamente me colaboraram e incentivaram a realização desse trabalho.

A Deus, por todas as oportunidades, novas chances e aprendizagens que apareceram na minha vida até hoje.

Meus pais, Luiz Fernando e Márcia, pelo exemplo de vida, conselhos, ensinamentos, apoio incondicional e amor que me amparam em todos os momentos de minha vida!

Ao meu irmão Thiago por ter seguido comigo, me suportando e incentivando sempre que necessário.

Ao meu avô Jorge e minha avó Jecileia por ter compreendido, mesmo na distância e saudade, sendo pilares e exemplos de vida que me apoiaram até agora com suas palavras.

Ao meu padrinho e madrinha, Maurício e Sandra, pelas palavras de motivação e ao meu afilhado Lucca pelos seus pensamentos e energias positivas.

Tia Maria, Tia Elma, Tia Jicelda, Tio Paulo, Tia Irei, Tia Catarina, Tio Miguel, Thaís, Tarcila, Luiza, Tia Sandrinha, Bilim, Kássia, Ademir, Miryam, Carlos Artur, Nézio, Lidiane, Cíntia, Marcelo, pelas palavras de apoio, pensamentos sempre positivos e momentos de alegrias e de boas risadas!

Ao Professor Alfredo, por ter encarado essa jornada com sua orientação, suporte e preciosos conselhos.

Ao Ronnie, por toda força (lá ele), suporte e conselhos em situações acadêmicas e pessoais.

Aos meus amigos e companheiros do grupo de inovação em engrenagem (GIE) André Maia, Patrícia, Lucas, Nico (Tonico), Filipe (Fofão), Vágner pelo suporte tanto pessoal quanto na realização desse trabalho.

Ao André Teixeira, pelas preocupações e todo suporte dispendido no entendimento da simulação híbrida mesmo lá das terras germânicas.

Aos meus amigos Matheus (Chunga), Douglas, André Lima (Superman), Luiz (Marombinha), Rafael (Cubo), Rafaela, Hudson, Sérgio (Velho), Glaucos, Cassiano, Cézar (Exótico), Donizete, amigos CCM, Viçosa e Cachoeiro pelas discussões (quase sempre de

fato discussões) técnico-científicas-filosóficas e conversas de boteco que apoiaram essa jornada.

"If we knew what it was we were doing, it would not be called research, would it?"

Albert Einstein

Resumo

Integridade superficial pode ser considerada como um dos parâmetros mais estudado devido aos seus efeitos no desempenho de um produto. Com isso, a relação entre funcionalidade e as variáveis de manufatura tem sido mapeados, principalmente para processos de usinagem, devido às influências dos carregamentos termomecânicos gerados na tensão residual induzida pelo processo. Assim, indústrias de manufatura com base em usinagem são naturalmente interessadas nesse ramo de investigação. Complementarmente, práticas sustentáveis estão sendo aplicada na usinagem, demandando a otimização das operações com o intuito de reduzir custos, redução de perdas do processo e ajustes ambientais, por exemplo, influenciando também em características funcionais do componente. Assim, a validação da integridade funcional tem sido cada vez mais requerida. Devido ao fato de processos experimentais serem demorados, métodos computacionais alternativos começam a ser considerados. Contudo, apenas abordagens numéricas ineficientes estão dispostas para processos de usinagem complexas. Desta forma, é necessária a proposição de uma abordagem numérica nova e eficiente. Uma possiblidade, baseada no método de elementos finitos, é a abordagem híbrida para processos de usinagem complexa. Essa abordagem pode ser resumida como a aplicação direta dos carregamentos da usinagem, sem a necessidade do modelamento das condições de interface peça-ferramenta. Contudo, esse método foi apenas testado para processos de usinagens simples, não sendo observado para processos mais complexos. Assim, esse trabalho propõe a aplicação do método híbrido para fresamento de topo. Essa aplicabilidade resultou uma redução substancial na resolução do modelo (de dias para horas) gerando os dados de saída desejados (campo de tensões residuais). Os desafios associados a esse método foram identificados como a medição e aplicação dos carregamentos, como também a correta definição das condições de contorno. Como segundo ponto, foi observado que o campo de tensões pôde ser calculado sem a obrigação de se aplicar os carregamentos na forma final do componente, deixando o modelamento da usinagem menos complexo. Desta forma, mesmo com as simplificações empregadas no modelo, a possibilidade de expansão para outros processos de usinagem foi confirmada.

Abstract

Surface integrity can be considered as a parameter that is most studied due to its effects on the product performance. The relationship between the functionality and manufacturing variable effects has been mapped, mainly associated with machining process. This process is focused on the connection among the thermo-mechanical loads generated during the process and the residual stresses induced by them. For that reason, industries that have the machining process as the base of the manufacturing chain are naturally interested in these investigations. Additionally, sustainable practices have been put in place, such that for cost reduction, loss reduction and environmental adjustments, optimization of the machining process is demanded. Therefore, validation of functional integrity is more and more required. As experimental procedures are time consuming, alternative computational methods are considered, but only inefficient approaches for complex machining operations are available. Thus, there is need to propose new and efficient one possibility, based on the finite element method, is a hybrid approach for complex machining processes. This approach can be described as the direct application of the machining loads in the workpiece without the necessity of modelling the interaction between tool and workpiece. However, that method was just tested for simple cases of machining, and the application for a more complex process has not been tried yet. Therefore, this work proposes the application of the hybrid method in the end-milling process. This approach resulted in substantial reduction of time for solving the model (from days to hours) with the desired outcomes (residual stress field). The challenges associated with this method were identified as load measurements and the application of these loads, and also the correct definition of the boundary conditions. Another point that was observed is that the residual stress field can be computed without the obligation to apply the loads in the finished shape. That fact renders the machining process easier to model. Finally, even with the simplification of the model, the possibility to expand for other machining processes was confirmed.

List of Figures

List of Tables

xv

List of Abbreviations

2D	Two-dimensional
3D	Three-dimensional
ANFAVEA	*Associação Nacional dos Fabricantes de Veículos Automotores*
AISI	American Iron and Steel Institute
ALE	Arbitrary Lagrangian Eulerian
BC	Boundary condition
CAE	Computer Aided Engineering
CCM	*Centro de Competência em Manufatura*
DIN	*Deutsches Institut für Normung*
FEM	Finite element method
ISO	International Organization for Standardization
ITA	*Instituto Tecnológico de Aeronáutica*
MATLAB	Numerical computation software from MathWorks
PSZ	Primary shear zone
RS	Residual stress
SAE	Society of Automotive Engineers
SSZ	Secondary shear zone
TSZ	Tertiary shear zone

List of Symbols

Symbol	Unit	Description
$(1-m_c)$	-	Angular coefficient of the curve specific cutting force versus chip thickness
A	MPa	Yielding stress
A	mm²	Cross section area
a	mm	Half of the length action
a_e	mm	Radial depth
B	MPa	Hardening factor
C	-	Strain rate constant
c	m/s	Sound speed in the material
[C]	N.s/m	Damping matrix
E	GPa	Elasticity (or Young's) modulus
F_c	N	Cutting force component
F_f	N	Feed force component
$F_{c\,(PSZ+SSZ)}$	N	Cutting force at primary shear zone and secondary shear zone
$F_{c\,(TSZ)}$	N	Cutting force parcel at tertiary shear zone
$F_{f\,(PSZ+SSZ)}$	N	Feed force parcel at primary shear zone and secondary shear zone
$F_{f\,(TSZ)}$	N	Feed force parcel at tertiary shear zone
fz	mm/tooth	Tooth feed
G	GPa	Shear modulus
h	mm	Chip thickness
K_s	kgf/mm²	Specific cutting pressure

$K_{c1,1}$	N/mm²	Specific cutting force
K	-	Empirical value to consider residual stress into the fatigue
[K]	N/m	Stiffness matrix
L_e	m	Effective length of the element
m	-	Temperature exponent
[M]	kg	Mass matrix
n	-	Strain hardening exponent
n	RPM	Spindle rotational speed
n_nodes	nodes	Quantity of nodes presents in the cutting zone
[N(x,y)]	-	Vector of interpolation functions
P_n	-	Cutting tool edge normal plane
p(x)	MPa	Pressure distribution
P	N	Normal force at surface
P_{th}	W	Thermal power diffused in the tertiary shear zone
$\vec{R}$	N	Resultant cutting force
{R}	N	External forces vector
T	ºC	Effective temperature
T_{melt}	ºC	Melting temperature
T_{room}	ºC	Room temperature
T_n	s	Smallest period of the finite element assemblage
t_c	s	Cutting period
$\{\ddot{u}\}$	m/s²	Acceleration vector
$\{\dot{u}\}$	m/s	Velocity vector
$\{u\}$	m	Displacement vector
v_c	m/min	Cutting speed

$\mu_{(SSZ)}$	-	Friction coefficient on interface tool-workpiece at secondary shear zone
α_n	o	Clearance angle
β_n	o	Wedge angle
γ_n	o	Rake angle
$\varDelta t$	s	Time step
Δt_{cr}	s	Critical time step
ε_{ij}	-	Strain components of the strain tensor
$\dot{\bar{\varepsilon}}$	1/s	Effective strain rate
$\dot{\bar{\varepsilon}}_0$	1/s	Reference strain rate
Λ_3	-	Repartition coefficient of heat flux
μ	-	Friction coefficient
μ_{app}	-	Apparent friction coefficient
μ_{plas}	-	Plastic friction coefficient
μ_{adh}	-	Adhesive friction coefficient
ν	-	Poisson's ratio
ρ	kg/m³	Density
σ	MPa	Normal stress
σ_{res}	Pa	Residual stress
σ_{act}	Pa	Acting stress
σ^{I}	Pa	First order residual stress
σ^{II}	Pa	Second order residual stress
σ^{III}	Pa	Third order residual stress
σ_a	Pa	Fatigue resistance considering residual stress

σ$_w$	Pa	Fatigue resistance without consider residual stress resistance
σ_{ij}	Pa	Stress components of the stress tensor
$[\sigma]$	Pa	Stress tensor
τ	MPa	Shear stress
τ_{crit}	MPa	Critical shear stress
Φ(x,y)	field unit	Field value for a non-nodal position
Φ$_i$	field unit	Field value for a nodal position
φ_c	rad	Engagement angle

Contents

1 Introduction

Surface integrity is the object of many studies today. The reason for that importance is the association between manufactured surface and the functional performance, which defines the surface integrity (ASTAKHOV, 2010). Thus, the understanding of the behavior and, mainly, the prediction of the factors associated with the surface integrity are much more understood and, for that, is increasingly used in manufacturing optimization.

The conjunction of the factors that compose the surface integrity can be directly correlated with the surface topography and surface metallurgy, which influences the fatigue strength of the component that was manufactured (JAVIDI, 2008), as sketched in Figure 1.
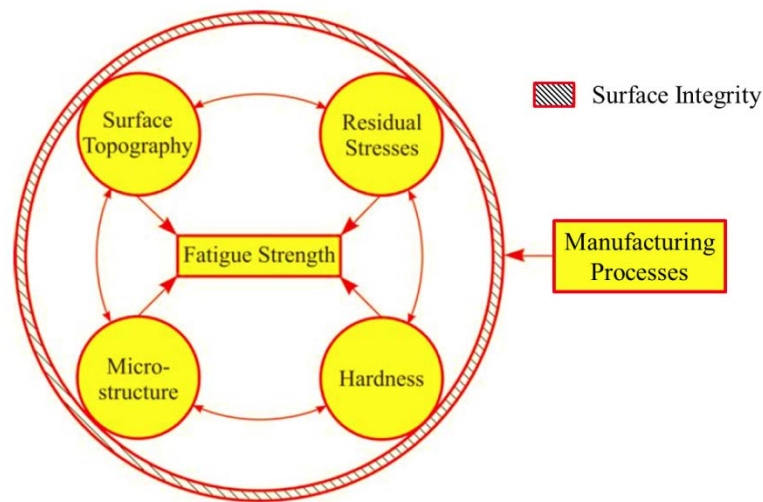
Figure 1 - Surface integrity factors network with its actuation in the fatigue strength (JAVIDI, 2008)

The control of these factors is fundamental to prevent fatigue failures. However some of these factors can be monitored and controlled more easily such as residual stress, for an industrial application. Javidi (JAVIDI, 2008) states that the residual stress and the surface topography are the surface integrity parameters that most interfere with fatigue control after machining process. The surface roughness can be controlled in a range of values depending on the process. Figure 2 shows the arithmetic average of the roughness profile R_a for basic machining processes.

Ra µm	50	25	12.5	6.3	3.2	1.6	0.8	0.4	0.2	0.1	0.05	0.025	0.012
Ra µin	2000	1000	500	250	125	63	32	16	8	4	2	1	0.5

METAL CUTTING
sawing
planning, shaping
drilling
milling
boring, turning
broaching
reaming
ABRASIVE
grinding
barrel finishing
hining
electro-polishing
electrolytic grinding
polishing
lapping
superfinishing

Figure 2 - Surface finish of basic machining processes (ASTAKHOV, 2010).

Typical defects such as cracks with sharp outlines can appear in machined surfaces (ASTAKHOV, 2010). These undesired effects cannot be predicted in general cases, being an uncontrollable parameter. Therefore, it is more acceptable to work on the prediction and control of residual stresses.

Regarding the combination between dynamic functioning (predisposition to have a fatigue failure) and the machining process, the gear is a component that must be carefully considered. It is observed that machining is one of the main processes that composes its manufacturing chain, as presented in Figure 3.
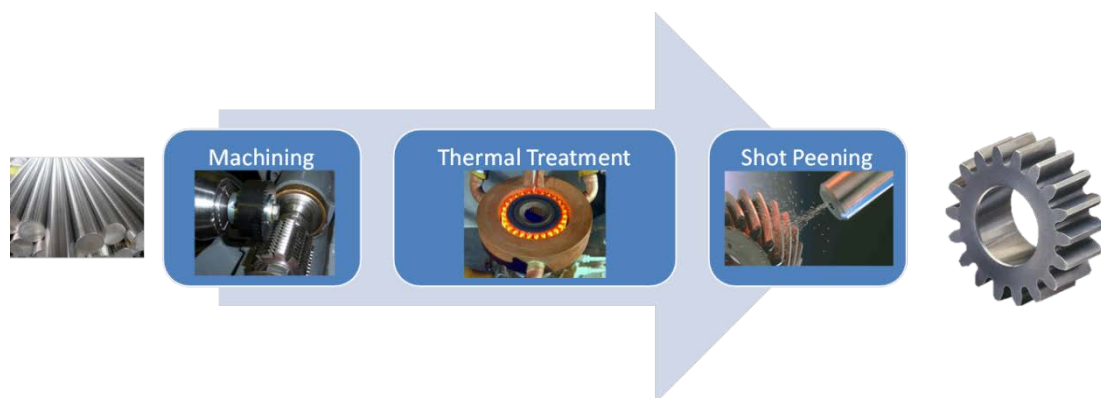
Figure 3 - Gear manufacturing chain (GUPTA *et al.*, 2016; REGO, 2011).

According to ANFAVEA, *Associação Nacional dos Fabricantes de Veículos Automotores*, only in Brazil in the last 5 years, the production of the light-duty vehicle was above of 15 million of units, almost 94% of the whole production in the same period, as shown in Figure 4.

Automobile Brazilian Production
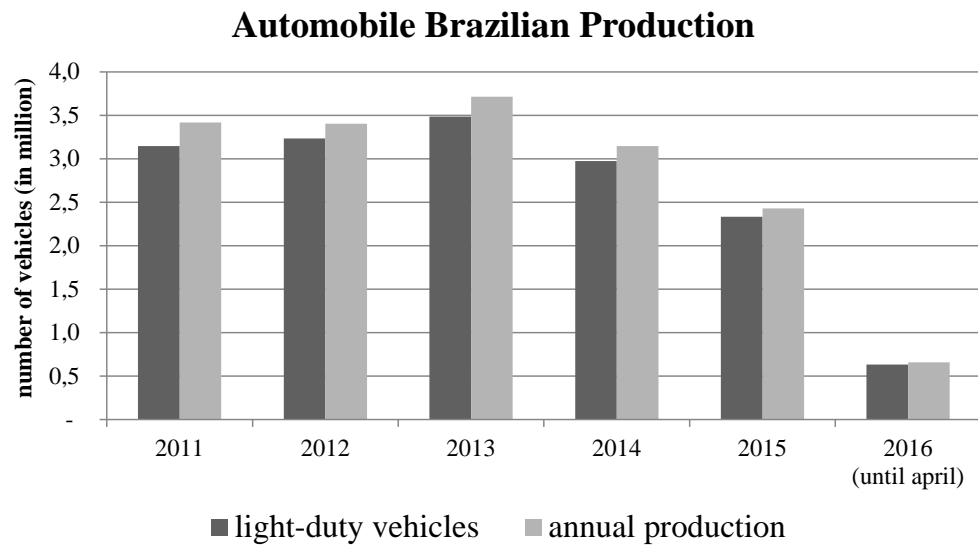
Figure 4 - Light-duty vehicle Brazilian production (ANFAVEA).

More than 180 million gears were produced to supply the Brazilian automobile industry. Having its manufacturing basis as machining process, the costs associated should to be high, because considering an overall production cost for the machining, 7-20% is related with lubri-cooling whereas 4% is related with cutting tools (SOUZA, 2014). Thus, the necessity to optimize the cutting parameters is always present, always looking for cost reduction. In addition, a sustainable tendency in the gear machining calls even more for optimization. Aspects as lubri-cooling method, material wasting during the process and energy consumption are some points that the sustainable manufacturing will address, ensuring not only the productivity and product quality, but also compliance to environmental sustainability and regulations (GUPTA *et al*., 2016).

Optimization is only possible if product reliability is maintained. That requirement is partly associated to the costumer, which is more demanding these days. Thus, the functionality must be satisfied and must not be changed. Since dynamic functionality and manufacturing processes are together defined as surface integrity, the way to validate these parameters is by the factors that can influence it.

The industrial capacity to control the residual stress induced by the manufacturing chain, adding a new process, is higher than to control the surface roughness. Moreover, the residual stress has its basis on three aspects: mechanical, thermal and microstructural. They are always presented in the machining. However, this validation is a time consuming task and expensive to be ran experimentally (ARRAZOLA *et al*., 2013). For that reason, the industry tries to find out an alternative method to predict the effects of residual stress that is

simultaneously cheap and fast enough. The numerical and analytical methods are candidates. Figure 5 presents the disadvantages of each alternative method.
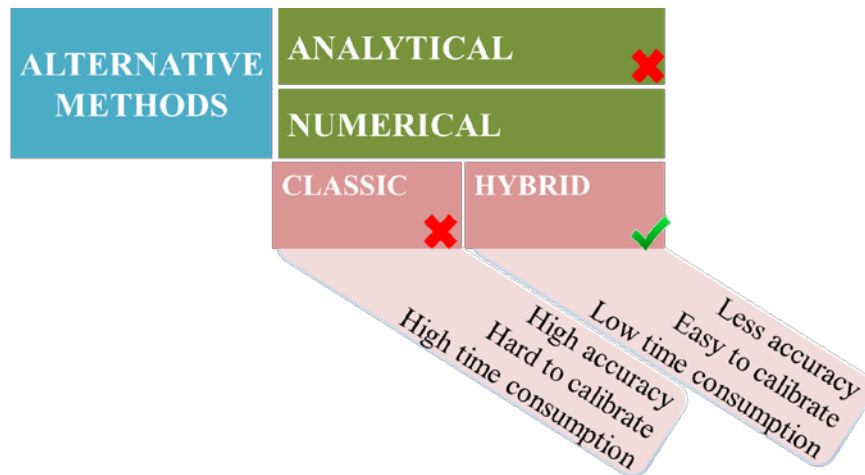
Figure 5 - Alternative methods and their disadvantages (ARRAZOLA *et al*., 2013).

The hybrid method is a possibility for the gear hobbing application. However, its applicability for milling must first be assessed. That must be done because it was just proposed and validated for the turning process not guaranteeing its applicability for other machining processes. The complexity is correlated with the use of the hybrid method for machining processes that do not generate a chip with constant shape, as in turning. Even the three processes are classified as machining with geometrically defined tool, by the DIN 8580, it exists the difference among their chip geometry, as shown in Figure 6.
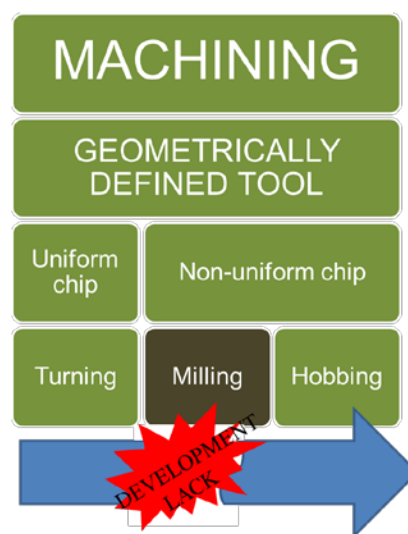
Figure 6 - Processes with their respective chip geometry.

If was proved that the hybrid method is just possible to machining processes that have uniform chip, the work to expand the approach to another machining process will not be more necessary. Thus, at first attempting, the hybrid method must be applied to the milling process.

This dissertation will present fundamental points of the residual stress modelling for the machining process. Aspects related to the following three subjects will be considered:

- Machining process (focused on milling);

- Residual stress (generated by the mechanical and thermal effects);

- Finite element method.

The discussion will be oriented in a numerical simulation direction, always observing the main objective of this work that is the physical validity of the outcomes. Thus, the way to certify the results to the milling process will be defined by the characteristic of the residual stress and by its peculiarities.

2 Objective

The main objective of the present work is to validate a non-conventional method, as known as hybrid method, to predict residual stress field induced by end-milling considering the thermo-mechanical effects.

The development of this work takes into account as principal technical concern the association between numerical simulations and machining process, in special end-milling process. In order to achieve the general objective, some specific objectives were defined. For each one, a way to evaluate if it was satisfied has been planned, as listed below:

a) Evaluation if the residual stress field obtained in the simulation is physically coherent:
   i.   Verification of the residual stress equilibrium.

b) Evaluation if the thermo-mechanical loads, provided by an experimental procedure or an analytical model, are representative to predict the residual stress field by itself:
   i.   Verification of the residual stress state in comparison with experimental data;
   ii. Verification of the temperature distribution after the cut.

3 Literature Review

3.1. Machining

3.1.1. General definition

The manufacturing processes are defined by their action in the raw material until achievement of the desired form, which could be the intermediate or final shape. DIN 8580, a German technical standardization, categorizes most of the processes in six groups related with the type of modification on the material, as shown in Figure 7.

Figure 7 - Manufacturing process definition (Based in DIN 8580).

All the machining processes belong, in that categorization, to group 3. A factor that is unique of that process is the generation of chips, which are material layers that are removed by the action of the tool during the contact, by consequences of the kinematic phenomena involved (KLOCKE, 2011; TLUSTY, 2000). Machining is then categorized as a volume reduction process.

Given the large range of ways that machining processes can be made, the placement of all processes in the same division may not to be a correct classification. Hence, two subdivisions were formulated, concerning the tool geometry, to englobe the different types of machining processes, as show in Figure 8.
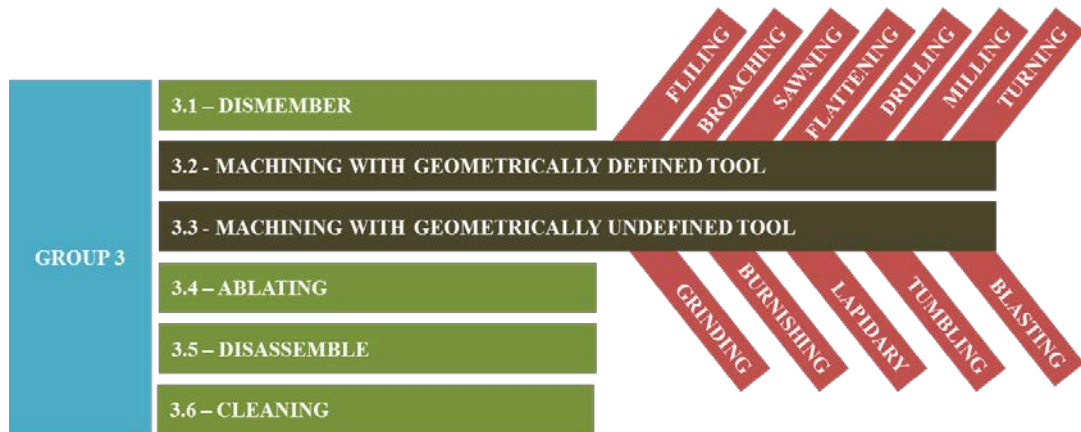
Figure 8 - Machining processes as a volume reduction type (Adapted from DIN 8580).

3.1.2. Tool geometry and shear angles

Considering that the relative motion that generates the chip is composed by the contact between two parts, the knowledge about their interaction must to be established. That dependency is because, during the formation of the chip, the behavior in the interaction that will dictate machining aspects such as tool wear, machining load (forces and temperature) generation, dynamic behavior of the process and chip geometry (DINIZ; MARCONDES; COPPINI, 2000; GOMES, 1996; KLOCKE, 2011).

The study of the interaction between the tool and workpiece involves the geometry of the cutter in association with the cutting variables that set the cutting process. Figure 9 presents the general concept of cutting wedge, which is defined by DIN 6581 and ISO 30021.
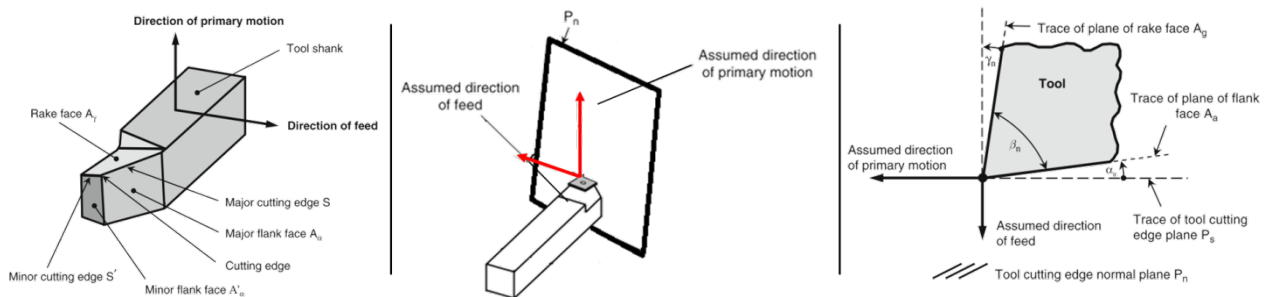
Figure 9 – General machining tool geometry and the wedge cut (Adapted from KLOCKE, 2011).

The geometry of a tool has different angles and edges that make its wedge, The three angles are present: γ_n rake angle, β_n wedge angle and α_n clearance angle. Moreover, that concepti shown in the Figure 9 is just an approximation, because the cutting edge is modelled

as a sharp angle. Considering the real geometry that is found in the tool wedge, it is possible to define another principle of the cutting: the shear zones. Figure 10 presents the idealized and real cutting edges.
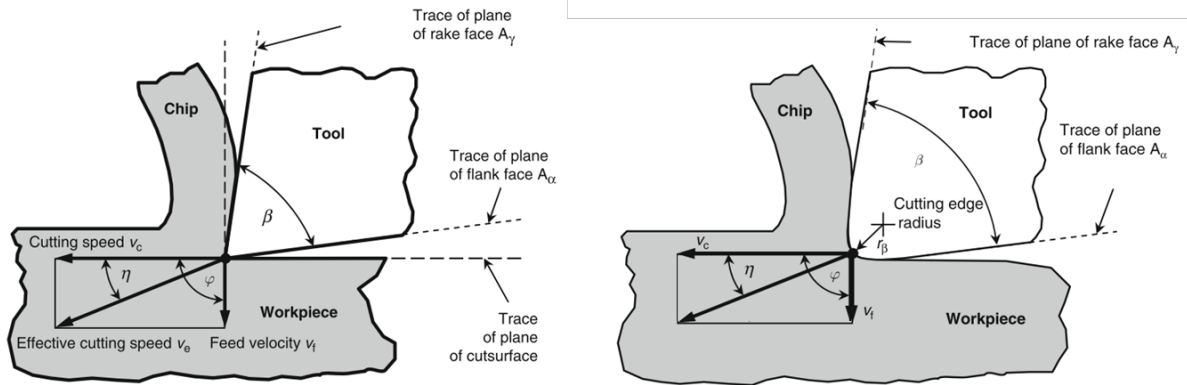
Figure 10 - Idealized and real cutting edge (KLOCKE, 2011).

The definition of the real cutting edge permits to visualize and understand the three shear zones that exist in the chip generation. As indicated in Figure 11 the primary shear zone (PSZ) is defined in zone *a*, where there exists the higher shear deformations in the material; *b* is the chip itself; *c* is the secondary shear zone (SSZ), also known as flux zone; *d* is the tertiary shear zone (TSZ), where the interface between the cut surface and the tool edge exists and *e* is the stagnation zone, where the highest compressive stress are present and also where the flow speed is almost zero.
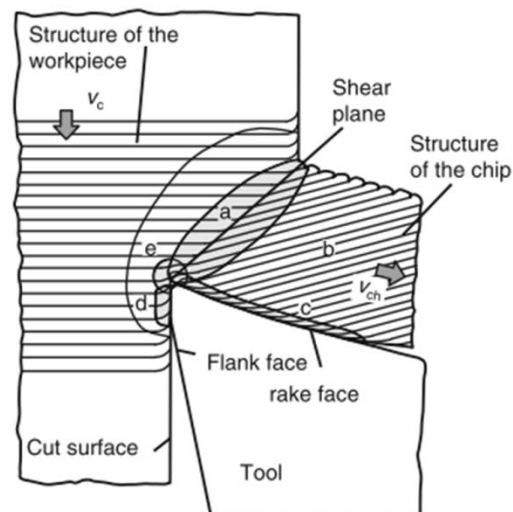
Figure 11 - Chip formation with the shear zones evidenced (KLOCKE, 2011)

3.1.3. Force and temperature

To a machining process, the loads are proportional to the chip thickness. Thus, a variation of the thermo-mechanical loads is proportional with the chip thickness variation (MAIA, 2015). According to Diniz (DINIZ; MARCONDES; COPPINI, 2000), there are at least two ways to study the forces in the machining: phenomenologically, by the study of the chip generation, and empirically, using specific equipment to measure the forces during the cutting process. The analytical form needs to have a certain precision to guarantee the correct representation of the process. Considering that the combination of the milling parameters associated with the material can interfere with the force profile that the process will generate, so the model must to be calibrated to a specific cutting process. The second one is associated with models that include cutting coefficients that must be calibrated by experimental results.

Considering the chip generation method to predict the cutting forces in the machining, equation 1 represents a relationship that can be used.

$$F_c = K_s A \qquad (1)$$

The value of K_s is defined as the specific cutting pressure and A is the cross section area of the chip. K_s depends on the combination of the workpiece composition and tool geometry and material, influencing mainly the friction coefficient in the interface chip-tool during the machining process (DINIZ; MARCONDES; COPPINI, 2000). Values for K_s can be found in tables and graphs for different materials.

A theory that can be expressed as empirical to find the cutting forces is proposed by Kienzle, represented by equation 2.

$$F_c' = K_{c1.1} h^{(1-m_c)} \qquad (2)$$

The value of $K_{c1,1}$ is defined as the specific cutting force that must be applied to remove a chip with undeformed width $b = 1$ mm and undeformed thickness $h = 1$ mm, also depending of the material on the tool and workpiece. The validity for the model is deeply related to experiments that are ran to calibrate the model. So, a variation in the cutting parameters leads to the necessity to recalibrate the model (MAIA, 2015).

The generated temperature during the machining process is due to the contact between tool and workpiece in the interfaces in the SSZ and TSZ. Each cutting variable has its effect

in the temperature, being the union of these effects the key to predict the heat generation during the process. The heat is dissipated in the interfaces that were shown in Figure 11. The percentage for each zone depends of many factors, such as the material that is cut, tool used for the process and also the cooling technique (DINIZ; MARCONDES; COPPINI, 2000). The Figure 12 presents that distribution according the cutting speed. But not only cutting speed influences the thermal distribution, being the material that is cut and also other machining parameters inducing great influences in the thermal distribution.
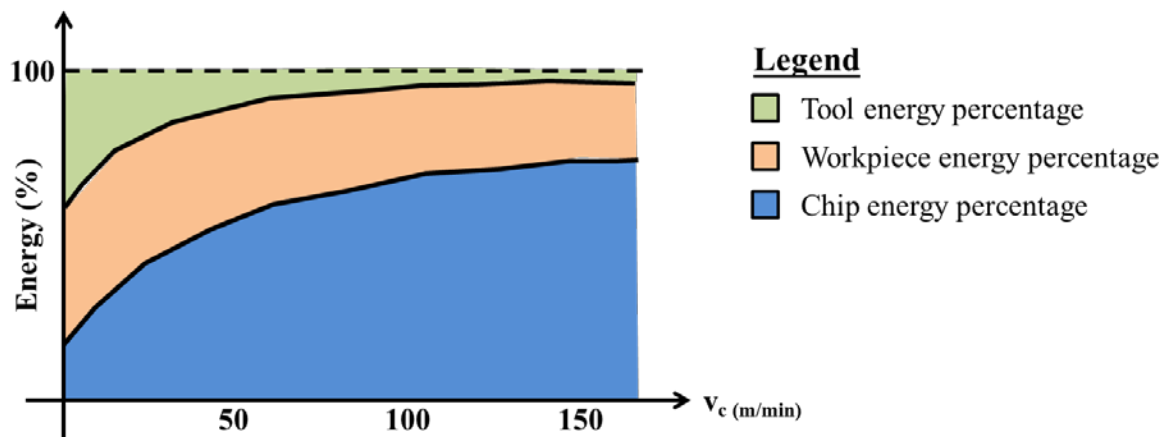
Figure 12 – Distribution variation of the energy in each part in function of the cutting speed (Adapted from DINIZ; MARCONDES; COPPINI, 2000).

3.1.4. Milling process

Milling is a machining process that is specially characterized by its kinematics. The tool, which is responsible for the rotating motion, has its cutting edges disposed symmetrically around its axis in most of cases. The feed motions are made by the table where the workpiece milled is mounted on. The classification of the milling can be made by the angle that is formed by the cutting tool axis and the surface generated after the process, being tangential when the angle equals 0º and frontal when the angle equals 90º, as shown in Figure 13.
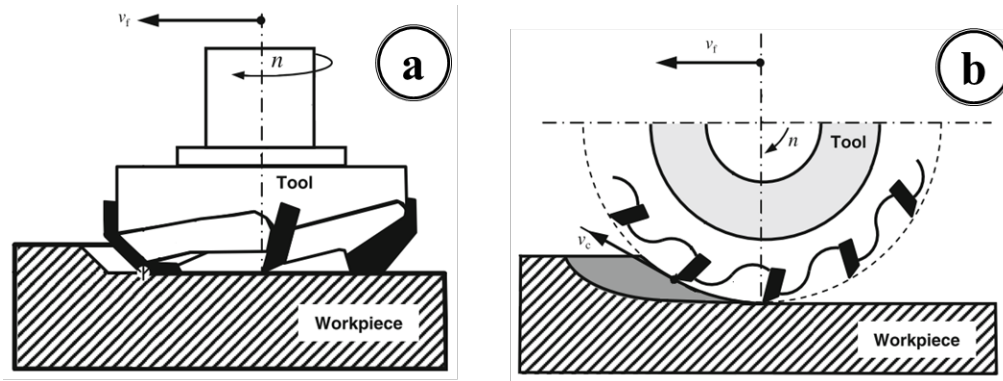
Figure 13 – Milling process classification a) frontal milling and b) tangencial milling (Adapted from KLOCKE, 2011).

For the tangential milling, according to the combination of the feed direction of the workpiece and the tool rotation motion, there are two possibilities to make this operation as shown in Figure 14. In all milling processes the tool engagement with the workpiece during the cut is not constant and changes each moment (KLOCKE, 2011). Two possibilities are shown in Figure 14.

Down milling   Up milling

■ Chip generated
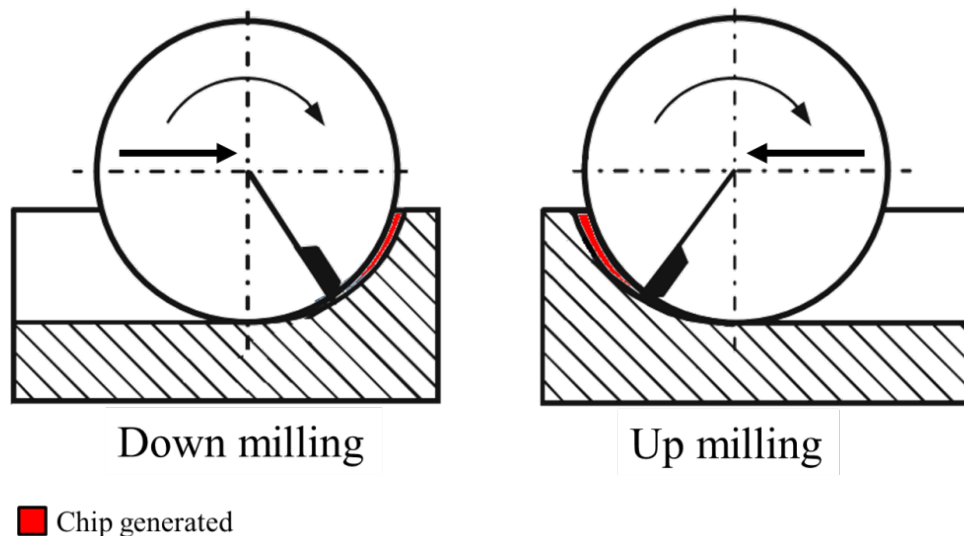
Figure 14 – Down and up tangential milling processes and their chip (Adapted from KLOCKE, 2011).

Up milling and down milling, with the same cutting variables, produce a comma-shaped chip with the same dimensions. However, during the generation process for the down milling, the chip begins to be formed with the maximum thickness (that equals tooth feed) until its minimum value (that equals zero). Up milling has the opposite behavior, changing the chip thickness from minimum to maximum value (DINIZ; MARCONDES; COPPINI, 2000). The direct consequence of that chip variation is the force induced by the process. For this

reason, there is a strong relationship between the force profile and the chip thickness generated. Therefore, the chip variation will lead to force variation.
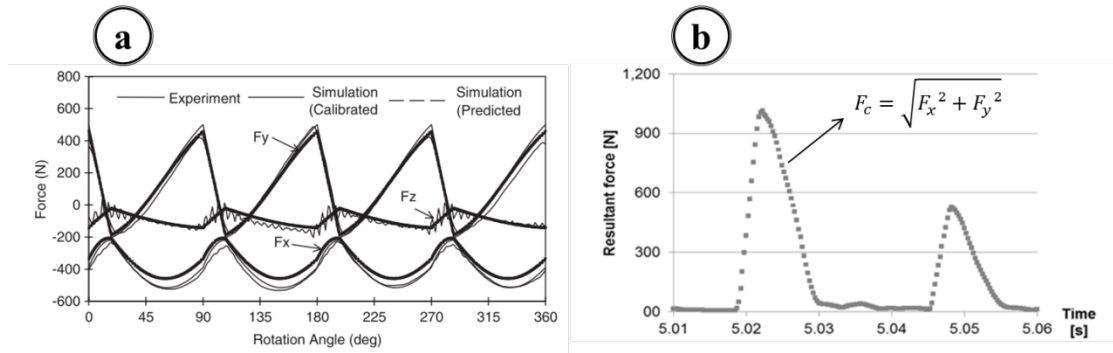
Figure 15 – Forces profiles for 4-flutes up milling (a) and 2 indexible inserts down milling (b) (BUDAK, 2006; adapted from MAIA, 2015, respectively)

3.2. Residual stress

3.2.1. Residual stress definition

Residual stress is a static triaxial stress field that a mechanical component is submitted without the action of external loads (LU, 2002; VALIORGUE, 2009). Moreover, it consists of an equilibrium stress state, as given by equation 3.

$$\int_V \delta\varepsilon\, \sigma_{res}\, dV = 0 \tag{3}$$

When an external force is applied to the component, the resultant stress field that will be in the part can be computed as the superposition of these two effects, for all the six independent terms of the stress tensor (LU, 2002), as shown in Figure 16.
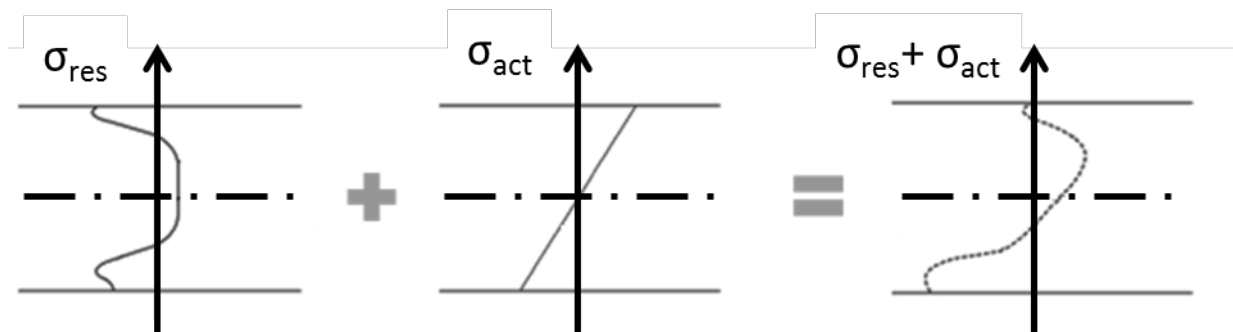
Figure 16 - Residual stress (σ_{res}), imposed stress (σ_{act}) and resultant stress ($\sigma_{res+}\sigma_{act}$) (Adapted from LU, 2002).

3.2.2. Residual stress types and origins

Residual stresses can be classified according to their actuation level in the material. These actuation levels are listed as macro, micro and atomic level, as shown in Figure 17.
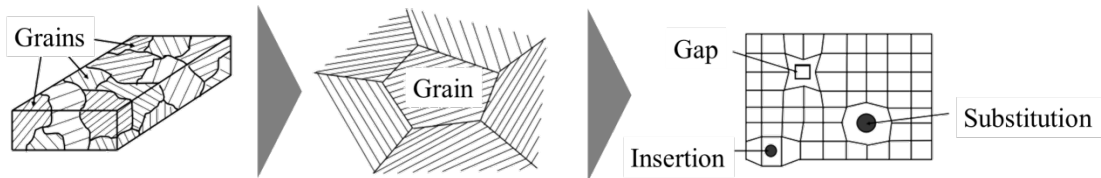
Figure 17 - Levels of the actuation of the three types of RS (Adapted from VALIORGUE, 2009)

For each level, a different order of residual stress is related. For the macro level, observed in large dimension of the material, the residual stress is classified as first order (σ^I). At a grain level (that can be expressed also with the phase), the residual stress is classified as second order (σ^{II}). And with an atomic level, the residual stress is categorized as third order (σ^{III}). Each one has its effects on general aspects on the component, such as dimensional variation, and the residual stress field to a piece is the superposition of the three types (VALIORGUE, 2009). The most accessible type, experimentally and numerically, is of the first order, being considered in many research lines.

Regardless of the type of residual stresses presents, their origins are related to three main factors: mechanical, thermal and chemical by the effects of deformation, temperature and microstructure of the material (BHADESHIA, 2002). These effects are generated by manufacturing processes that the material is submitted to. Lu (2002) indicates that the residual stress expresses a manufacturing process history that a mechanical component has passed by in its whole manufacturing chain, being necessary to know the process that the component is submitted to understand the residual stress that is generated. Thus, each process has its influence in the residual stress field. These influences can appear isolated or in combination (VALIORGUE *et al.*, 2007). The Table 1 presents some manufacturing processes and their effects on the residual stress for each factor (Lu, 2002).

Table 1 - Some manufacturing processes and their residual stress effects (Adapted from LU, 2002)

PROCESS	RESIDUAL STRESS ORIGINS		
	MECHANICAL	THERMAL	STRUCTURAL
Casting	No	Temperature gradient	Phase transformation
Shot peening, hammer peening, roller bunishing	Plastic deformation with gradient (surface to core)	No	Depends on the material
Grinding, turning, milling, drilling, boring, ...	Plastic deformation due to the chip removal	Temperature gradient due to local heating	Depends if temperature is sufficiently high
Quenching without phase transformation	No	Temperature gradient	No
Surface quenching with phase transformation	No	Temperature gradient	Change of volume due to a phase change
Case hardening, nitriding	No	Thermal incompatibility	New chemical component with volume modification
Welding	Shrinkage	Temperature gradient	Microstructural change
Brazing	Mechanical incompatiblity	Thermal incompatibility	New phase at interface

3.2.3. Fatigue life influenced by residual stress

The residual stress is one of the factors related to the surface integrity of a manufactured component. Its effects are related to the surface integrity of a manufactured part because it can alter many parameters related to the crack propagation being beneficial or not. These effects can be expressed as initialization, propagation and increase of the rate that a crack is propagating or barring, retarding and decreasing the crack propagation rate (LÖRE, LANG, VÖHRINGER, 2002). The compressive state of residual stress is the most beneficial for the surface integrity for its effects against the crack propagation (FONSECA, 2015). For that, post treatment after the manufacturing chain such as shot peening or deep rolling are used to guarantee the beneficial residual stress field for the fatigue strength (FUNATANI, 2002; FONSECA, 2015; REGO, 2011)).

As a function of the residual stress, the fatigue limit that the material presents can be expressed as indicated in equation 4 (JAVIDI, 2008).

$$\sigma_a = \sigma_W - K\sigma_{res} \qquad (4)$$

The value σ_W is the fatigue resistance without the presence of residual stress. The K, an empirical factor that depends of the mechanical properties of the material, varies from 0.1 to 0.3, having its highest value typically for materials with high strength (JAVIDI, 2008). So, the fatigue behavior and its prediction are only completely understood when the residual stress and also the stress caused by the external loads are known. As it was shown in Figure 16, the stress field that is induced by the external load must be considered when the stress analysis is made. In fact, with the action of the same process to improve the fatigue strength, the effect of the residual stress that is generated can be more beneficial to one component than another. Lu (2002) presents a table, shown in Table 2, which demonstrates the increase of the fatigue life, in different mechanical components, with the effect of the residual stress generated by the shot peening process.

Table 2 - Increasing of the fatigue strength made by the shot peening process in different mechanical components (LU, 2002).

Type of part	Type of stress	Increase in the fatigue life (%)
Spindles	Reverse bending	400–1900
Shafts	Torsional	700
Gear box	Fatigue life tests in service	80
Crankshafts	Fatigue life tests in service	3000, but highly variable
Aircraft coupling rods	Tensile compression	105
Driving rods	Tensile compression	45
Cam springs	Dynamic stress	100–340
Helical springs	Fatigue life in service	3500
Torque rods	Dynamic stress	140–600
Universal joint shaft	Reverse bending	350
Gear wheel	Fatigue life tests	130
Tank chain	Fatigue life tests	1100
Weld	Fatigue life tests	200
Valve	Fatigue life tests	700
Rocker arm	Fatigue life tests	320

3.3. Finite element method

The finite element method is a numerical approach that was developed to solve physical models that are considered too complicated to solve exactly, specially because of geometrical complexity (HUTTON, 2004). For that, an approximate solution is proposed to

replace the exact mathematical model (BATHE, 1982; HUTTON, 2004; RAO, 2004). The origin of this method is, according Rao (2004), in 1956, with the aim to be applied in the aerospace industry. Reinforced by Soriano (SORIANO; LIMA, 2003) the beginning of the use of this method was at 1955, with the modelling of the stress distribution in plates used in aircraft wings.

The problems that are solved by this method are classified as boundary value problems, which can be described as a mathematical problem where dependent variables, governed by differential equations in a domain defined by independent variables, must satisfy boundary conditions that are imposed in the domain frontier (HUTTON, 2004; RAO, 2004). Examples of physical problem that can be solved by finite element method are equilibrium problems, eigenvalue problems and transient problems (RAO, 2004).

Models that use finite element method are progressively in use in engineering activities, particularly due to computational advances and also the engineering modernization.

3.3.1. Global formulation

The exact solution of the mathematical problem, defined according to the physical problem, for the entire domain is a time consuming task, due to the geometrical complexity. Thus, instead of solving the mathematical model for the whole domain, which is supposed to be continuous, the solution is obtained just for discrete points of the domain, called nodes. Moreover, the mathematical problem that is solved is an approximation of the differential equation. For the points of the material that are not coincident with the nodes, the field values are determined, as shown in Figure 18, by an interpolation of the nodal values.
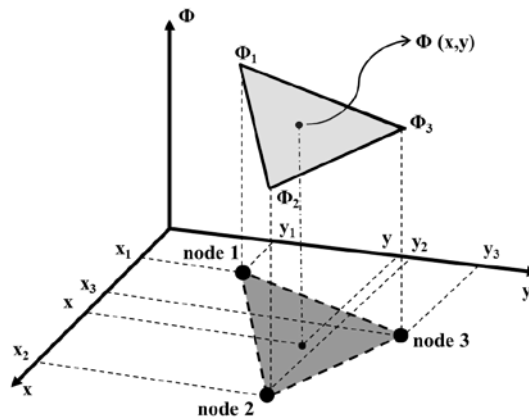
Figure 18 – Triangular element with 3 nodes in a two-dimensional model (Adapted from RAO, 2004).

Equation 5 indicates the interpolation for a two-dimensional model with triangular element with three nodes (HUTTON, 2004).

$$\phi(x, y) = [N]\{\phi\} = N_1\phi_1 + N_2\phi_2 + N_3\phi_3 \tag{5}$$

where ϕ_i and $N_i(x,y)$, being $i=1,2,3$, are the field nodal value and interpolation functions, respectively. The number of fields values that will be calculated in the domain is equals the number of degrees of freedom, that is defined as the product of number of nodes in the model and the number of field variable that each node has (HUTTON, 2004)

The discretization of the model, in commercial finite element programs such as Abaqus, Nastran, Ansys is made by their specific algorithm, taking off the obligation of the user to generate the mesh. However, depending on the geometry complexity, some guidelines and knowledge of the user may be required to the correct adequacy and control of the mesh (RAO, 2004).

Considering that, in the finite element method the solution is made only for the nodal points, the quality of the results is deeply related to the discretization level. In Figure 19-a, a quadrangular element with a coarse mesh is shown. Between nodes #1 and #2, the field variable is known by an interpolation as it was represented in equation 5. However, if the same domain was discretized with a mesh that has its elements with a half size, as it is shown in Figure 19-b, the results can change. That is because a new node appears between the node #1 and the ancient node #2, introducing a solved field variable in a place where there was interpolation before. If, between the two nodes in Figure 19-a a high gradient is present in the field value, its effects will not be noted.
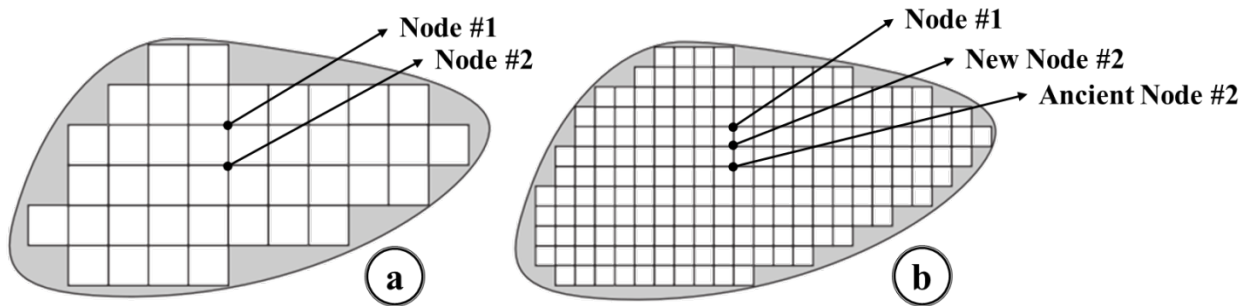
Figure 19 – Model discretization of a domain: a) Domain less discretized b) Domain more discretized (Adapted from HUTTON, 2004).

To avoid that issue with the model discretization, the convergence of the model is made to guarantee that the mesh size does corrupt its outcomes. The procedure is to refine, reducing the element size until the variation of a field value achieve a specific tolerance. Thus, the results obtained can be expressed as corresponding to the exact solution (HUTTON, 2004; SORIANO; LIMA, 2003). Although the accuracy of a model is related to a highly discretized domain, the large number of nodes in a model induces a large number of degrees of freedom, which requires more computational capacity to solve the equations (RAO, 2004). Thus, a ponderation with the discretization level and computational cost must be made during the convergence study.

3.3.2. Explicit formulation

To solve dynamic equations in a nonlinear analysis, the finite element method uses, in general, three groups of algorithms: incremental, iterative, and time integration algorithms. (BATHE, 1982). For the last group, two approaches are employed: the explicit integration and implicit integration. The explicit integration uses a direct integration method to find the equilibrium of the dynamic system governed by the equation 6.

$$[M]\{\ddot{u}\} + [C]\{\dot{u}\} + [K]\{u\} = \{R\} \tag{6}$$

where *[M]* is the mass matrix, *[C]* is the damping matrix, *[K]* is the stiffness matrix, $\{\ddot{u}\}$ is the acceleration vector, $\{\dot{u}\}$ is the velocity vector, $\{u\}$ is the displacement vector and *{R}* is the external forces vector. This method is called direct because it does not use any kind of transformation before the numerical integration (RAO, 2004). Differently from the implicit method, the explicit method does not use the stiffness or damping matrices (FONSECA, 2015).

The explicit integration uses, in most cases, the central difference method, a direct integration method. With this approach, the displacement at time *t+Δt* is computed with the equilibrium of the equation system at time *t* (BATHE, 1982). The disadvantage associated with the central difference method is related with its stability. To assure stability, a time step size *Δt* must be smaller than a critical time step value Δt_{cr}, that is (BATHE, 1982):

$$\Delta t \leq \Delta t_{cr} = \frac{T_n}{\pi} \tag{7}$$

Where T_n is the smallest period of the finite element assemblage with n degrees of freedom. A way to calculate the value of Δt in a model of a bar submitted by a constant step load is given by following equation (BATHE, 1982).

$$\Delta t = \frac{L_e}{c} \tag{8}$$

where L_e is the effective length of the element and c is the sound speed in the material, which can be calculated as indicated in the equation 9 (BATHE, 1982).

$$c = \sqrt{\frac{E}{\rho}} \tag{9}$$

where E is the Young's modulus and ρ is the density. The value that is obtained by equation 8 is interpreted as the time for the propagation of a wave in a media with the effective length equals L_e. The result of equation 8 is in accordance with the stability criteria established in the equation 7, being a possible time step value. Considering a finite element analysis, L_e can be considered as the smallest distance between two nodes in the mesh. (BATHE, 1982). Therefore, including the factor of the small elements introduces computational costs due to increasing of the degrees of freedom, this also causes the reduction of the time step for explicit approach if it was used.

An artificial way to bypass the issue of small elements in an explicit simulation is using the mass scaling. That factor is used to change, artificially, the density in order to increase the time step value (FONSECA, 2015).

3.3.3. Material non-linearity

A structural analysis can present three types of non-linearity: material, geometrical and boundary condition. The material type is where the material presents a behavior that extends beyond the elastic regime, having plastic deformation associated with the loads. To represent correctly the elasto-plastic behavior for a material the following parameters must be known:

- Elastic behavior (for an isotropic material):
    - Elastic modulus – E;
    - Possion's ratio – v;
    - Shear Modulus – G.
- Plastic behavior (BATHE, 1982):
    - Yield function;
    - Hardening rule;
    - Flow rule.

For the first group, the case was simplified to an isotropic material, where the elastic properties do not change with the direction that the material is loaded. That elastic behavior is present for polycrystalline materials, such as metal alloys. Only a pair of these properties must be known, because only two of them are independent (SORIANO; LIMA, 2003). The relationship to find the other one is shown in equation 10.

$$G = \frac{E}{2(1+v)} \tag{10}$$

Using the Voigt notation, the stress-strain relationship for an isotropic linear elastic material submitted to a general three-dimensional deformation is presented as equation 11 (HUTTON, 2004; RAO, 2004; SORIANO; LIMA, 2003).

$$\begin{Bmatrix} \varepsilon_x \\ \varepsilon_y \\ \varepsilon_z \\ \gamma_{yz} \\ \gamma_{xz} \\ \gamma_{xy} \end{Bmatrix} = \begin{bmatrix} 1/E & -v/E & -v/E & 0 & 0 & 0 \\ -v/E & 1/E & -v/E & 0 & 0 & 0 \\ -v/E & -v/E & 1/E & 0 & 0 & 0 \\ 0 & 0 & 0 & 1/G & 0 & 0 \\ 0 & 0 & 0 & 0 & 1/G & 0 \\ 0 & 0 & 0 & 0 & 0 & 1/G \end{bmatrix} \begin{Bmatrix} \sigma_x \\ \sigma_y \\ \sigma_z \\ \tau_{yz} \\ \tau_{xz} \\ \tau_{xy} \end{Bmatrix} \tag{11}$$

For the plastic behavior, the three properties must be known to be well characterized. The yield function or yield surface is the first element that and is defined as a function determined by the state variables that permits the plastic material characterization, as shown in equation 12 (BATHE, 1982).

$$f([\sigma]) = 0 \qquad\qquad (12)$$

Where f is the yield function (or yield surface) and $[\sigma]$ is the stress tensor. The yield surfaces are plotted in the principal stress space, existing a range of surfaces proposed, such as Tresca, von Mises, Mohr-Coulomb and Drucker-Prager (CRISFIELD, 1997). Each type is more recommended for a group of materials for their plastic behavior. Figure 20 shows Tresca and von Mises yield surfaces plotted in the stress space.
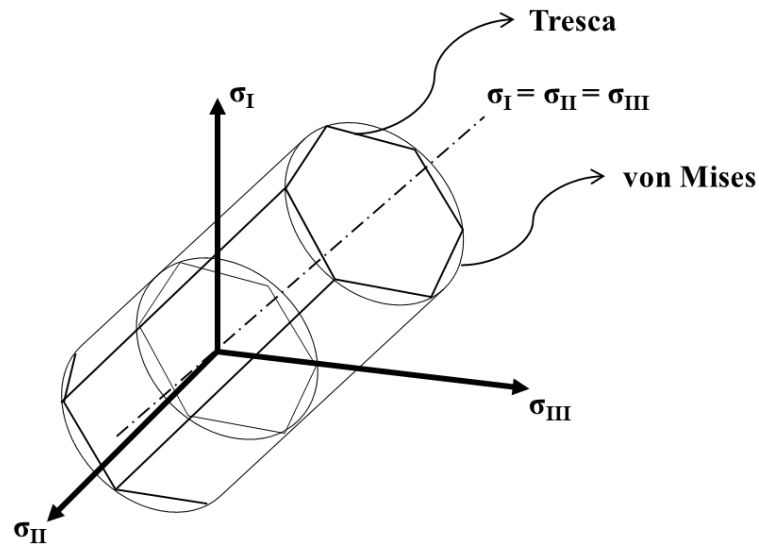
Figure 20 - Tresca and von Mises yield surfaces in the stress space (Adapted from CRISFIELD, 1997).

While a stress state inside the yield surface is possible, being characterized when the material is in its elastic behavior, the stress state cannot be defined outside the yield surface When the loading condition induces the stress state to be outside the yielding surface, it will change the yield surface according to the hardening rule (BATHE, 1982).

The hardening rules can be defined by two types: isotropic and kinematic, that defines how the yielding surface will change during the plastic flow. The isotropic type is characterized as a growth of the yielding surface with the same amount in all directions (FONSECA, 2015). Looking, in parallel, the stress-strain curve associated with the material, with the isotropic hardening law the variation of the yielding stress is the same for the tensile and compressive paths, as shown in Figure 21-a. However, with the kinematic type, the size of the yielding surface remains the same, having just a change of the location of the surface. With the same comparison with the stress-strain curve, the distance between the tensile and

compressive yielding stress remains the same, only having a motion with the hardening of the material, as represented in Figure 21-b. A mixed hardening law also exists, combining the two other types. The type of hardening depends of the material that is placed in a plastic behavior due to the loading that is submitted.
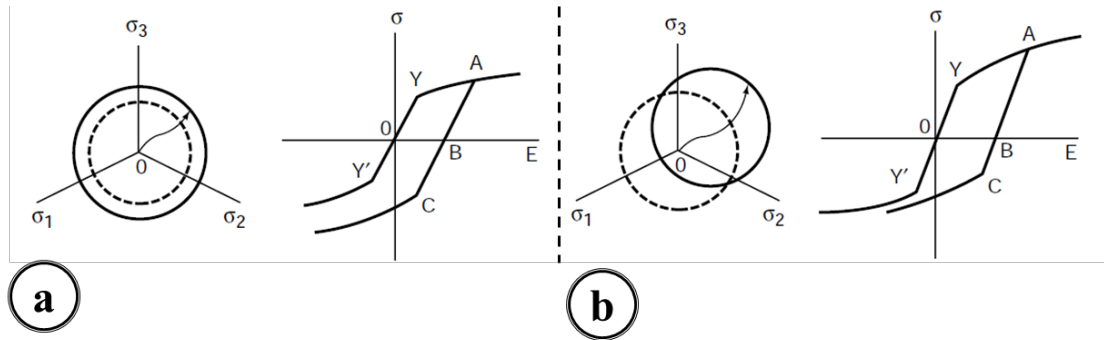
Figure 21 - Yield surface and stress-strain curves for hardening law explanation. Case a – Isotropic hardening law; Case b – Kinematic hardening law (INOUE, 2002)

The flow rule represents the association between the variation of the plastic strain $\{\varepsilon^{pl}\}$ and the variation of flow potential G as a function of the stress $\{\sigma\}$. Equation 13 presents the relation between these variations.

$$d\{\varepsilon^{pl}\} = d\lambda \frac{\partial G}{\partial\{\sigma\}} \tag{13}$$

If the flow is considered as associated, the plastic strain varies in a normal direction to the yield surface (FONSECA, 2015). However, the flow can be also considered as non-associated, being the direction of the plastic strain variation not commonly normal to the yield surface (CRISFIELD, 1997). That behavior is presented in materials such as cast iron in tensile loading, when brittle behavior is evident, and also with geomechanical materials (CRISFIELD, 1997).

3.4. Residual stress simulation for machining process

3.4.1. Classical model

The machining has been investigated, by many study lines, using numerical simulation with finite element method (ARRAZOLA *et al*., 2013). Following the advance of the computational capacity in the last decades, the possibility to simulate complex models was opened, permitting the creation and development of areas to apply that technology (ARRAZOLA *et al*., 2013; RAO; DANDEKAR; SHIN, 2011; SHET; DENG, 2000). Some of these research fields can be characterized as prediction of cutting forces and temperature (CERETTI *et al*., 2000; ÖZEL, 2006; RAO; DANDEKAR; SHIN, 2011), prediction of the chip generation (CALAMAZ; COUPARD; GIROT, 2008), tool wear/life (CERETTI *et al*., 2000), and surface integrity (JACOBUS; DEVOR; KAPOOR, 2000; MUÑOZ-SÁNCHEZ *et al*., 2011; STYGER; LAUBSCHER; OOSTHUIZEN, 2014).

For that purpose, a method as known as classical was proposed. In a nutshell, this method is a machining process made numerically, with the presence of the tool and the workpiece. However, this method is a highly demanding task to model and to solver the model (VALIORGUE *et al*., 2007). The interaction, with the relative motion between the parts exists and the chip is generated after the simulation by this approach, as shown in Figure 22 in a 2D and 3D model.
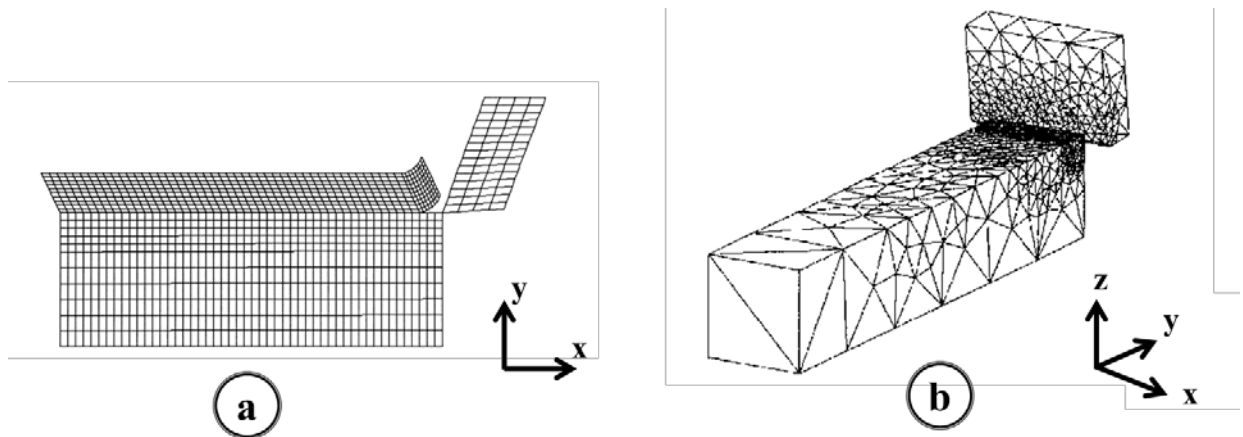
Figure 22 - Classical modelling in a 2D (figure a - (SHET; DENG, 2000)) and 3D (figure b - (CERETTI *et al*., 2000)).

The complete modelling has to consider many details to achieve the desired outcomes. These principal topics will be commented below to create a path of all the challenges that are present in that kind of modelling.

3.4.1.1. Constitutive property

The material definition is a factor that is deeply related to the machining process. In this manufacturing operation, the material where the cut happens , near the failure zone, has a combination of strain, high strain rates (10^2 to 10^6 1/s) and gradient of temperature (JASPERS; DAUTZENBERG, 2002; RAO; DANDEKAR; SHIN, 2011). Hence, a model that does not include these three parameters, as a conventional method using an universal testing machine, will not be a model recommended for this kind of simulation and could generate a wrong outcome for the machining modelling (JASPERS; DAUTZENBERG, 2002; ÖZEL, 2006).

Therefore, a model that is most applied for the machining simulation has the plasticity related to three terms that are: strain, strain rate and temperature (KLOCKE, 2011). One of the most used models is the Johnson-Cook model (GUILLEMOT *et al*., 2011), which was proposed in 1983, that describes the behavior of materials at high strain rates with thermal softening effects, as shown in Figure 23.
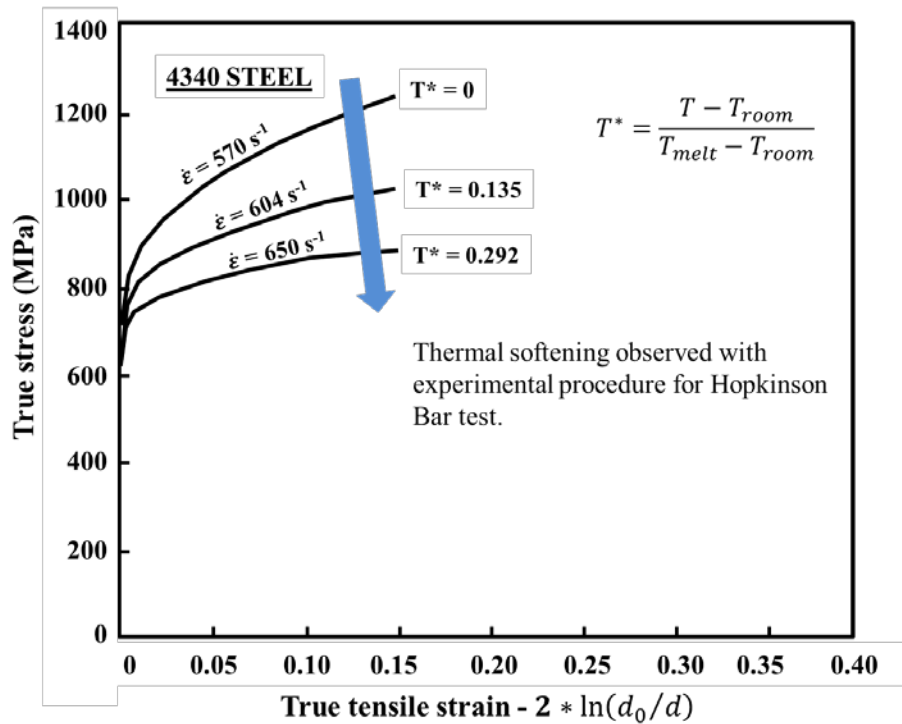
Figure 23 - Stress-strain curves for 4340 steel obtained for Hopkinson bar test with temperature variation. (Adapted from JOHNSON; COOK, 1983).

This model was proposed for computational application and was initially used in the ballistic field. The thermo-visco-plastic formulation that describes the flow stress to a material in this approach is shown in equation 14 (JOHNSON; COOK, 1983).

$$\overline{\sigma} = \left[A + B(\overline{\varepsilon})^n \right] \left[1 + C \ln\left(\frac{\dot{\overline{\varepsilon}}}{\dot{\overline{\varepsilon}}_0} \right) \right] \left[1 - \left(\frac{T - T_{room}}{T_{melt} - T_{room}} \right)^m \right] \qquad (14)$$

where A is the yielding stress (MPa), B is the hardening factor (MPa), n is the strain hardening parameter, $\overline{\varepsilon}$ is the effective strain, C is the strain rate constant, $\dot{\overline{\varepsilon}}$ is the effective strain rate (in 1/s), $\dot{\overline{\varepsilon}}_0$ is the reference strain rate (in 1/s), T_{room} is the room temperature (ºC), T_{melt} is the melting temperature (ºC) and T is the effective temperature (ºC). That constitutive equation is interpreted as a hardening law to the material and its classification is as isotropic hardening (DASSAUT SYSTÈMES, 2011).

Styger (STYGER; LAUBSCHER; OOSTHUIZEN, 2014) has presented a study comparing three different constitutive models, taking predicted cutting forces, temperature and residual stress as comparison aspects. He presents, as shown in Figure 24, the constitutive curves to Ti-6Al-4V utilizing the Johnson-Cook model, submitted to traction in different room temperatures and strain rates, evidencing the real influence of these parameters in the material behavior.
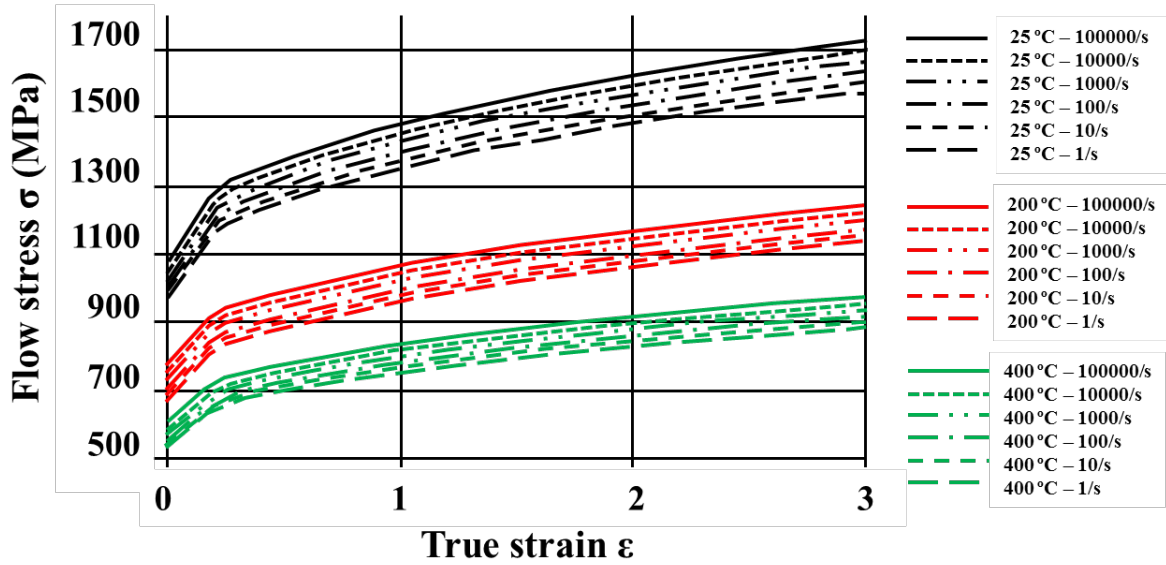
Figure 24 - Jonhson-Cook model curves for Ti-6Al-4V in different temperatures and strain-rates. (Adapted from (STYGER; LAUBSCHER; OOSTHUIZEN, 2014)).

The machining is a process that has, at the same time, elevated plasticity (until the material failure) and also high deformation (KLOCKE, 2011). Hence, to the correct modelling of the whole process, it must be considered two types of nonlinearities: the material (by the

constitutive equations) and the geometric (by including high-order terms in the strain-deformation relationship.

It must be noted that the classical model involves the presence of the workpiece and also the tool. All the discussion previously presented, applies only to the material that will be cut. The consideration about the tool material is simpler than that for the workpiece material because its mechanical resistance is higher compared to the workpiece. Some models can include wear mechanisms to predict that behavior for the tool, expanding the utilization of this technique (KLOCKE, 2011). However, if the objective of the model is just to investigate parameters related to the workpiece material, the tool could be considered as a rigid body for the CAE model.

3.4.1.2. Meshing

The meshing technique used to obtain the outcomes in a machining modelling is another point of relevance. First of all, specific treatment of the meshing was necessary because of high strains in the mesh. For that, computational methods such as adaptive meshing and automatic remeshing were used to help in this challenge (ARRAZOLA *et al*., 2013; RAO; DANDEKAR; SHIN, 2011). The application of these techniques was fundamental to the numerical convergence and to provide the evolution of this approach (ARRAZOLA *et al*., 2013).

Moreover, near the contact tool-workpiece zone, another factor related to the mesh can be found: meshing refinement. Due to the shear zone, that can appear in the chip formation, and also to the temperature gradient near of the cutting zone, the necessity to have the meshing refinement, associated with remeshing techniques, is clear (MOVAHHEDY, 2000).

A 2D example of a meshing design is presented in Figure 25, in an undeformed condition and some results that are entirely related to the discretization near the secondary shear zone.
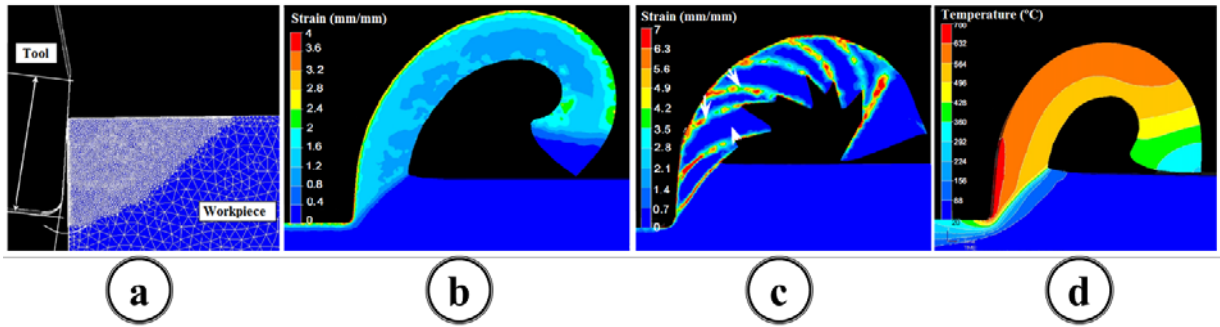
Figure 25 - a) Meshing technique used on a classical machining model; b) strain field in a non segmentated chip; c) strain field in a segmentated chip; d) Temperature distribution during a machining (Adaptation of CALAMAZ; COUPARD; GIROT, 2008).

Another point concerning the meshing technique is the meshing formulation. In the finite element method there are three ways to discretize a continuum media: Langrangian formulation, Eulerian formulation and Arbitrary Lagrangian-Eulerian (ALE) formulation. The first formulation is used in solid problems and has its nodes associated with the material points. For that, the mesh is sensitive to the high strain and, when it occurs, a remeshing rule must be applied, as shown in Figure 26 (ARRAZOLA; ÖZEL, 2010; KLOCKE, 2011; MOVAHHEDY, 2000).
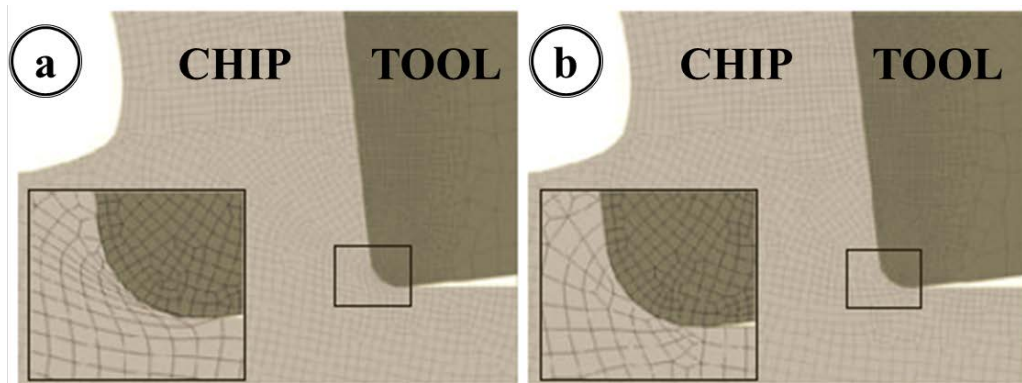
Figure 26 - Meshing behavior in a Lagrangian formulation. a) Distorted mesh, next to the tool edge radius, with possibility to have elements degenerated; b) Mesh after remeshing procedure, next to the tool edge radius, with controlled element distortion. (Adapted from (KLOCKE, 2011)).

The second approach is commonly used for fluid media and the nodes are not associated with the material points, disconnecting the material and mesh strain. However, at the unconstrained zones, that formulation is not the most appropriated to model (ARRAZOLA; ÖZEL, 2010; MOVAHHEDY, 2000). For all that reasons, the ALE formulation was proposed, because it will combine the advantages of these two formulations

(KLOCKE, 2011; MOVAHHEDY, 2000). In Figure 27, a model 2D with this approach is shown.
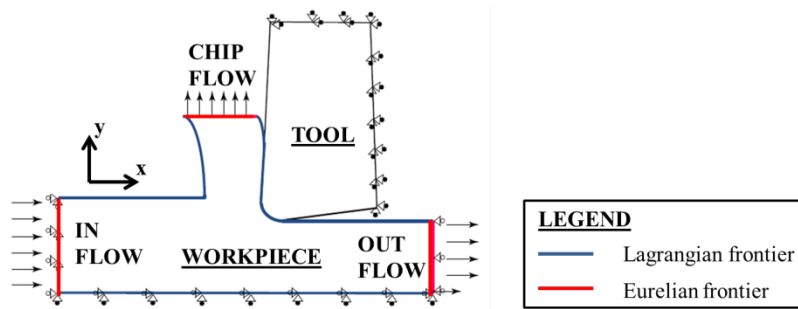
Figure 27 - Example of a 2D model with ALE formulation applied. (Adapted from ARRAZOLA; ÖZEL, 2010).

3.4.1.3. Load description

In the classical model, the load description is not an input data but only a consequence of the tool-workpiece contact, allowing the use of this method for a force prediction. So, this behavior represents an important role in the machining process, in the physical sense (SHET; DENG, 2000). For the action of very high normal pressures applied by the tool, that cutting parameter is influenced by the cutting variables, such as cutting speed, and feed rate (CERETTI *et al*., 2000). Thus, the interaction between the two parts must be known and its understanding is related as one of the challenges in this modelling of machining process (MUÑOZ-SÁNCHEZ *et al*., 2011).

The friction laws are most used to modelling the interaction in the interface tool-workpiece. The most common model is the Coulomb law that relates, in the machining, the shearing stress and the normal stress, by equation 15.

$$\tau = \mu\sigma \qquad (15)$$

where τ is the shear stress (MPa), σ is the normal stress (MPa) and μ is the friction coefficient at the interface. That ratio can be found by empirical procedures, with sliding test as indicated by (ARRAZOLA; ÖZEL, 2010) or by cutting experiments, using analytical models with experimentally obtained cutting forces, as (SOO; ASPINWALL; DEWES, 2004) made in its works with 3D modelling with Inconel 718.

Two regions can be described in the cutting zone, near the cutting edge: the sliding and the sticking region. As long as the shear stress is below of the critical value ($\tau < \tau_p$), a relative motion between the chip and the tool does not exist, configuring the sticking zone

whereas, when the shear stress exceeds the critical value, the chip motion will occur, as presented in equation 16 (SHET; DENG, 2000).

$$\tau = \min(\mu\sigma(x), \tau_p) \tag{16}$$

The τ_p value is related to the material failure (ZOREV also called that stress as average shear flow stress). Therefore, the equation 16 is only used to model the friction behavior in the sliding region (ZOREV *apud* ÖZEL, 2000), as shown in the Figure 28.
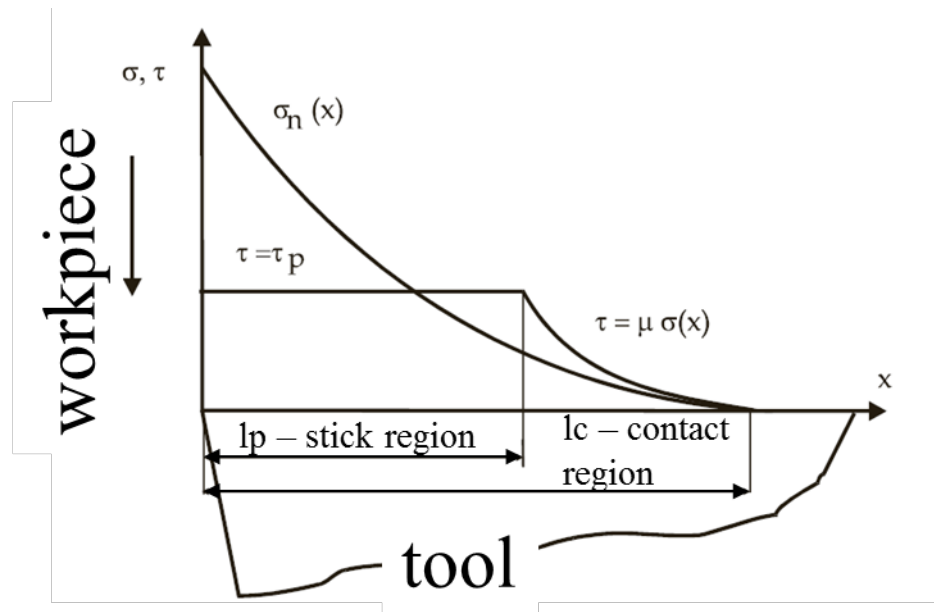
Figure 28 - Sliding and sticking region in a machining modelling. (ÖZEL;ZEREN; 2007).

3.4.2. Hybrid model

The hybrid model applied for the turning modelling was proposed by Valiorgue, in 2009, in his doctorate thesis. In substitution of the contact and the simulation of chip generation, this approach applies the thermo-mechanical load directly at the finished surface, as shown in Figure 29 (VALIORGUE, 2009).
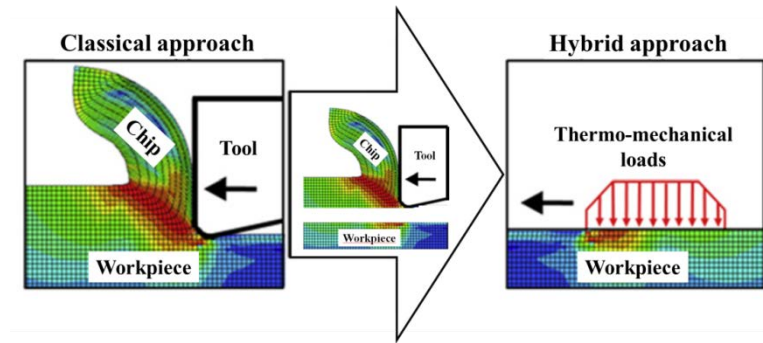
Figure 29 - Substitution proposed in the hybrid model with comparison with the classical model. (MONDELIN *et al*., 2012).

For the finite element method, the problem is not interpreted as a displacement described problem (description of the tool motion, in respect with the machining kinematic) and is taken as a force described (description of the load and its motion in respect with the relative motion between tool-workpiece).

This method has its advantages when compared to the classical model, in the prediction of residual stress, because the requirements that are needed to achieve the chip generation are a time consuming task. For example, a milling simulation with about 360,000 elements processed in a bi-processor with 3.21 GHz demanded about 10 days to be solved (MAUREL *et al*., 2008). However, the hybrid approach has the disadvantage to require a large data volume (experimental or simulation) for its input (ARRAZOLA *et al*., 2013). Guillemot consolidated in his thesis (GUILLEMOT, 2010) the advantages and disadvantages, shown in the Table 3, among the classical approach, analytic and hybrid, concluding that the hybrid method, even not being the most representative predictive method, has the best relationship between performance and time consumption.

Table 3 - Advantages and disadvantages of approaches to simulate residual stress (GUILLEMOT, 2010).

Approach	Physical model representation	Time consumption	Outcome precision	Experimental identification
Classical	+ + +	1 to 2 weeks	+ + +	High
Analytical	-	Seconds	+ +	Low
Hybrid (VALIORGUE, 2008)	+ +	Minutes	+ +	Medium

Valiorgue has validated the hybrid method, in completion for his proposal. That was made with experimental data of stainless steel SAE 316L, closing the whole cycle of a CAE modelling. Another use that was found with hybrid method was with prediction of temperature distribution in ball-tool milling (GUILLEMOT *et al*., 2011) with the prediction of residual stress also.

The hybrid approach can eliminate some difficulties that are found in the classical method. These differences and also the peculiarities of the hybrid approach will be presented in the next subsections.

3.4.2.1.   Common points between classical and hybrid approaches

These two methods have some similarities because, even with the difference in the approach, the modelling is of the same manufacturing process. The points in common between them are:

- **Constitutive property**: The material that represents the workpiece has the same behavior as function of the strain, strain rate and temperature in both methods. For that reason, the use of the Johnson-Cook model or other model that represents this behavior in high strain can be used;

- **Meshing**: Even not having the contact in the simulation, the meshing must be also refined in the hybrid method, mainly next to the surface where the load will be applied. It is necessary because the residual stress has a high gradient in that zone as well as the temperature (VALIORGUE, 2009). Thus, in order to avoid interference of the meshing size in the results, the mesh has to be refined.

3.4.2.2.   Load definition

The load definition is where the hybrid method has its main differences with the classical method. If the two approaches are compared, in the load definition aspect, the challenges to define just changed. The chip generation and meshing issues are replaced by the choice and the measurement of the loads that must be applied in the workpiece (VALIORGUE, 2008), as shown in Figure 30.
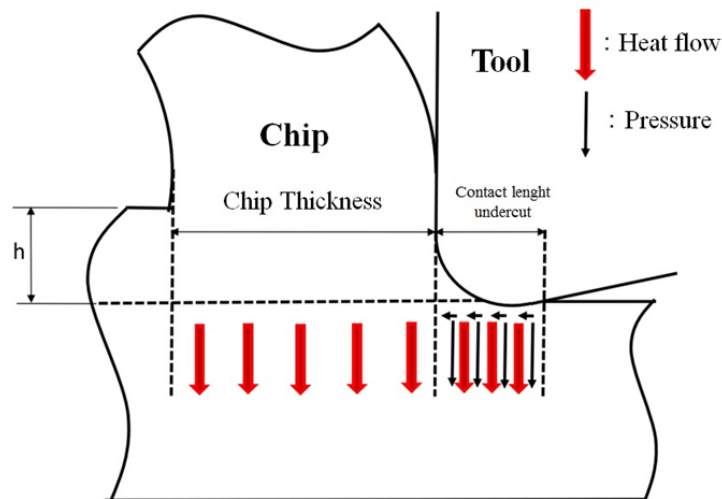
Figure 30 - Mechanical and thermal loads and their location in the cutting zone (VALIORGUE, 2008).

So, the understanding of the loads to be applied is the point that must be known. That understanding must be split in two parts (mechanical and thermal) to render that study easier.

The load modelling presented here is based in the study of Valiogue, because he has proposed the application of hybrid method for turning. However, in 2010, the residual stress prediction in an end-ball milling case was also studied, by Guillemot (GUILLEMOT, 2010). But, he also referenced Valiorgue in its load definition. For that reason, only the main reference will be considered.

The mechanical load is based on the distribution of the forces in the shear zones. Each of them has a parcel of this load and its contribution is:
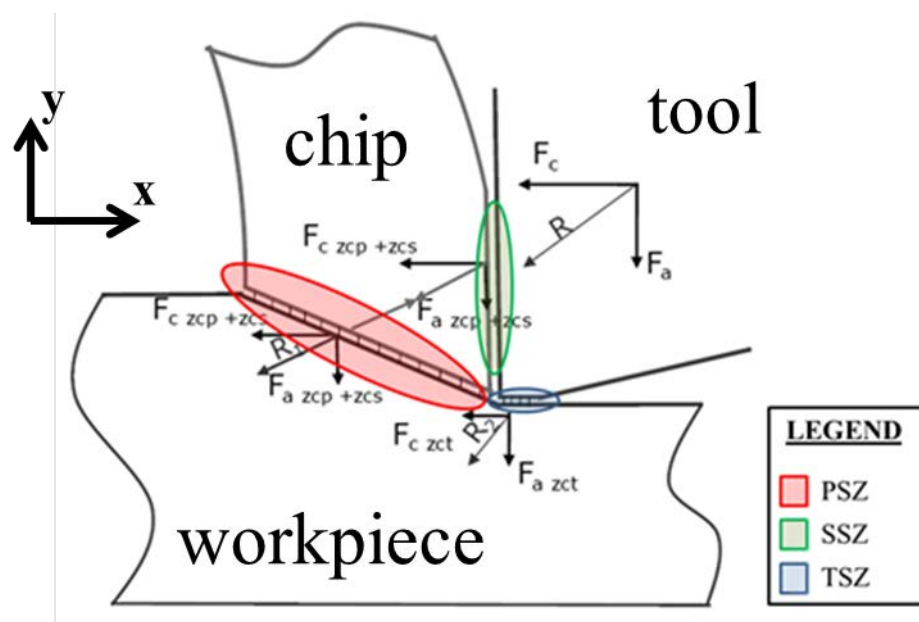
Figure 31 - Shear zone and its force parcels. (Adapted from (VALIORGUE, 2009)).

Supposing that the moments of the cutting forces are negligible, due to the application points to be small, the application of the force balance, based in the forces showed in Figure 31, leads to the expression:

$$\vec{R} = -(F_c \vec{i} + F_f \vec{j}) = -[(F_{c(PSZ+SSZ)} + F_{c(TSZ)})]\vec{i} + (F_{f(PSZ+SSZ)} + F_{f(TSZ)})\vec{j}] \qquad (17)$$

The feed force F_f that acts in the primary and secondary shear zones and also the cutting force F_c that acts in the tertiary shear zone are due to the friction phenomena in the tool-workpiece interface. That fact permits to write the relationship between the feed force and the cutting force in that zones by the friction coefficient as described by the Coulomb law, as shown in equations 18 and 19.

$$F_{f(PSZ+SSZ)} = \mu_{(SSZ)} * F_{c(PSZ+SSZ)} \qquad (18)$$

$$F_{c(TSZ)} = \mu_{(TSZ)} * F_{f(TSZ)} \qquad (19)$$

The friction coefficients are not directly found and need to have a specific method to discover. That is because, in the machining process, the friction coefficient that can be found by the general forces (that are measured by piezoelectric platform), is the apparent friction coefficient, the sum of the adhesive and plastic coefficients, as shown in equation 20 (VALIORGUE, 2009).

$$\mu_{app} = \frac{F_t}{F_n} = \mu_{plas} + \mu_{adh} \qquad (20)$$

In that sense, just the adhesive part represents in fact the interaction in the contact tool-workpiece (VALIORGUE, 2009). To determine that portion of friction coefficient, an experimental procedure simpler than the machining process was made. The steps to that determination, according Valiorgue, are:

- Tribological procedure to measure the normal and tangential forces in a tribometer;
- Finite element analysis to obtain the adhesive friction coefficient parcel to use in the mechanical load prediction.

A specific kind of tribometer was used in that measurement. It has an association with a dynamometer with a pin of carbide with TiN coating and a thermistor to measure the heat flux during the experimentation. With the auxiliary of the FEM, the adhesive parcel and also the heat flux is found with the model of a pin in contact with a piece, in a 3D model. Figure 32 presents the experimental and simulation tribological procedures.
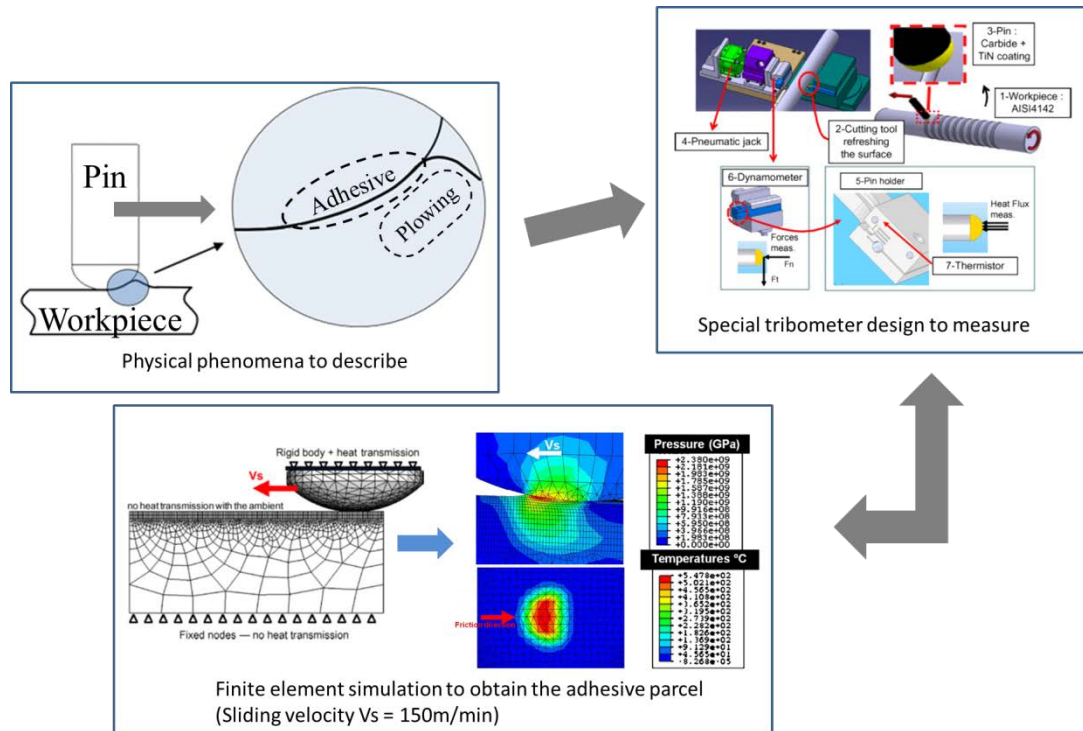
Figure 32 - Experimental and numerical procedures to obtain the adhesive friction coefficient and heat flux (adapted from RECH; CLAUDIN; D'ERAMO, 2009; VALIORGUE, 2009; ZEMZEMI *et al*., 2009).

That interaction between the numerical simulation and the experiment is done iteratively until the outcomes obtained in the numerical simulation coincide with the experimental results, as presented in Figure 33. When all the comparisons achieve the convergence, the value of the adhesive parcel and the heat flux in the workpiece material can be considered as obtained.
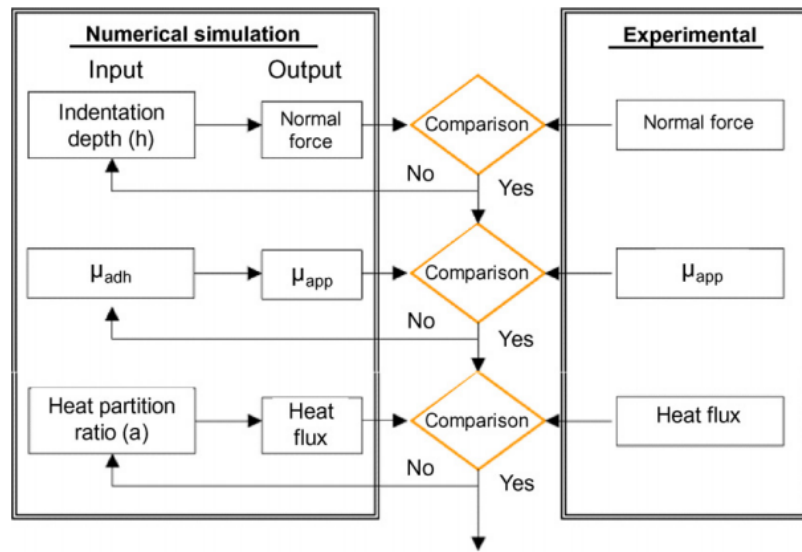
Figure 33 - Procedure to compare the numerical and experimental outcomes to obtain the values adhesive parcel and heat flux (ZEMZEMI *et al*., 2009).

Ending the description for the mechanical load, the pressures (normal and shear) due to the forces applied at the TSZ are calculated with the Hertz elastic contact theory, of a contact between a plane and plane (GUILLEMOT, 2010; VALIORGUE, 2009), described in Figure 34.

Pressure distribution:
$$p(x) = \frac{2P}{\pi a^2} * \sqrt{(a^2 - x^2)}$$
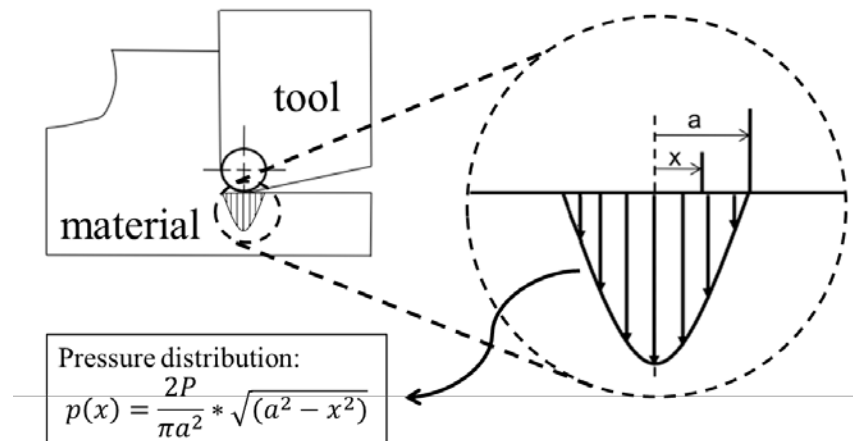
Figure 34 - Pressure distribution in the tertiary shear zone (Adapted from VALIORGUE, 2009).

where *p(x)* is the load value at an *x* position (MPa), *P* is the load that will generate the pressure (N). In that modelling, *P* will assume the value of $F_{f\,(TSZ)}$ to calculate the normal pressure and $F_{c\,(TSZ)}$ to obtain the shear stress. The value *a* is the half of the action of the pressure and the *x* is the position to be found the value of the pressure, both in (mm).

The thermal load is, in some part, related to the previous method, because the repartition of heat flux $Λ_3$ for the heat parcel that will be diffused in the workpiece material was already acquired. The heat that will be generated by the cutting power propagated in the TSZ is determined as described by equation 21.

$$P_{th} = \Lambda_3 \mu_{TSZ} F_{f(TSZ)} v_c \tag{21}$$

Thus, to obtain the loads that were applied in the hybrid method for turning, one must know (VALIORGUE, 2009):

- Experimental cutting forces F_c and F_f;
- Chip thickness h;
- Dimension a for the contact between tool and workpiece in TSZ;
- Coefficient of heat repartition $Λ_3$;
- Adhesive friction coefficient at the SSZ and TSZ.

4 Method proposal

The methodology applied during the development of this work was guided by the flowchart shown in Figure 35.
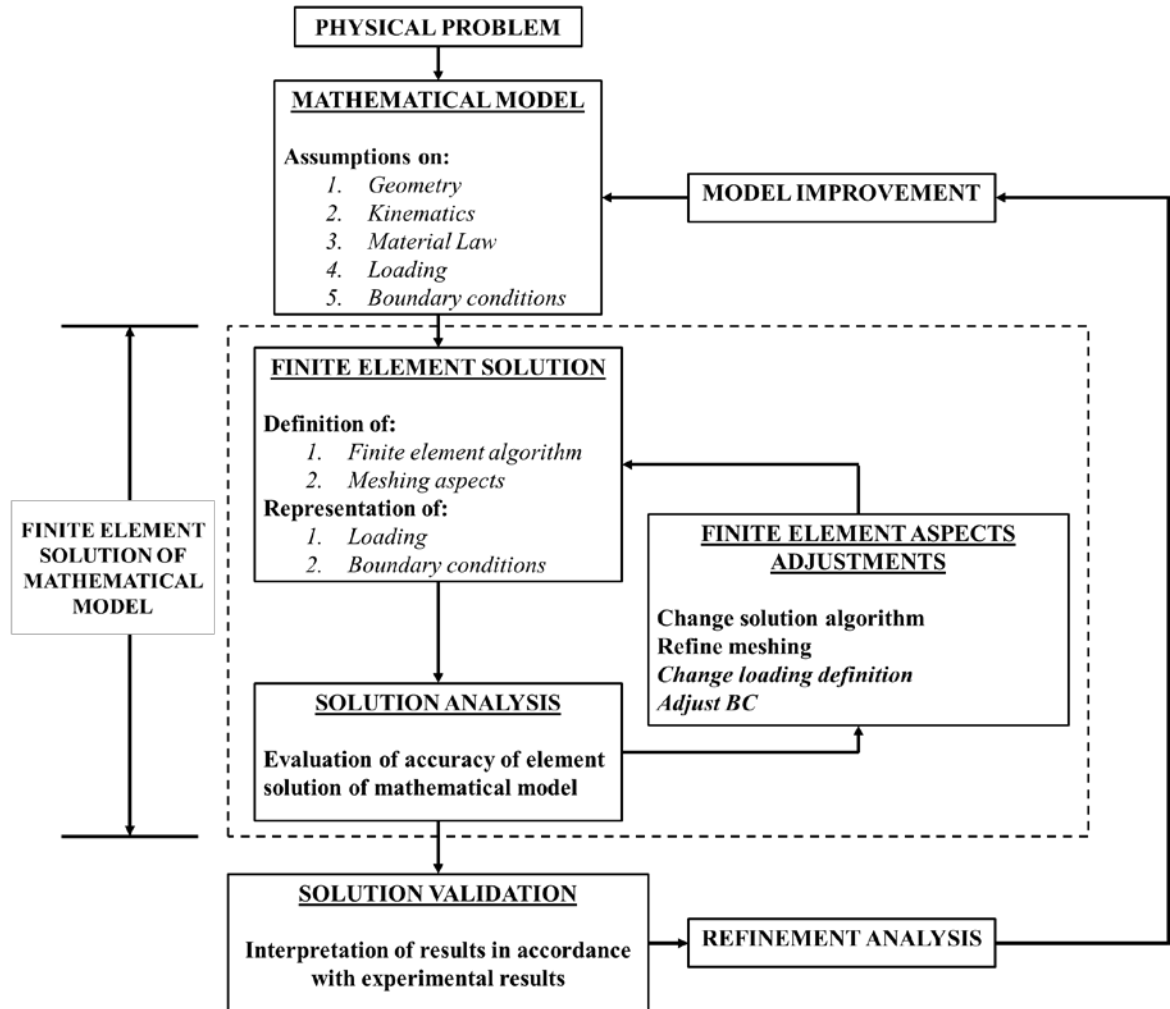
Figure 35 - General flowchart of a finite element analysis – (Adapted from BATHE, 1982).

The flowchart is considered as a general guide for any finite element analysis, because all the main steps included in that kind of analysis are contemplated. Every single part of the FEM sequence solution is fundamental for the correct representation of the physical model and, after the conclusion of the model, either physical or numerical parameters can influence the results obtained. In this chapter, only the *Mathematical Model* and *Finite Element Solution* will be addressed. *Solution Analysis* and *Solution Validation* will be addressed in the chapter *Results and Discussion*.

Valiorgue's study (VALIORGUE, 2009) was considered as a baseline to the development. However, some points related to the force definition and its application was different in order to try another way to use the hybrid method.

4.1. Physical problem

Although milling and turning are considered as a defined geometrically tool, the kinematics of these two processes are different. For turning, the relative motion between the tool and the workpiece is made by the rotation of the workpiece in conjunction with the in-plane translation of the tool whereas for milling the tool rotates combining with the in-plane translation of the workpiece, as shown in Figure 36.
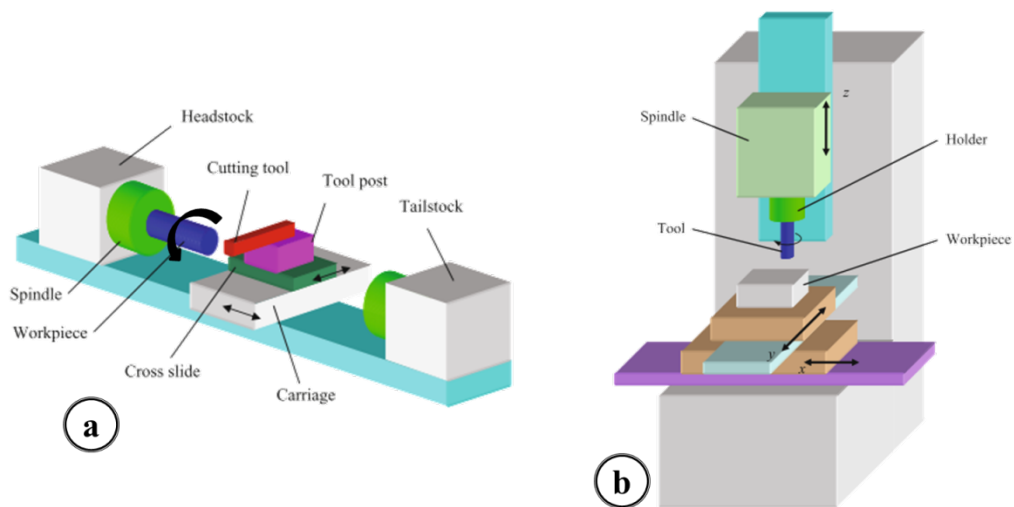
Figure 36 - Differences between the kinematic of turning (figure a) and milling (figure b). (Adapted from SCHMITZ; SMITH, 2009).

Moreover, the milling process is a multipoint cutting process, that is, not only a single point makes the cutting during the process. Thus, whereas the chip is constantly generated as in the turning, the milling produces a variable chip thickness in each passage of the tool, leading to differences in the milling in the hybrid model, because the loads will change in association with the chip thickness change.

4.2. Model assumptions

4.2.1. Geometric assumption

For the application of the hybrid method to the end milling operation, some details were observed in the reference method, proposed by Valiorgue (VALIORGUE, 2009). The geometry of the whole model (that is, in the hybrid method proposed by Valiorgue for turning and by Guillemot for end-ball milling) is considered as the final shape, without the chip

presence. Thus, that approach leads to know how the forces and temperatures will be distributed in the finished surface, as indicated in Figure 37.
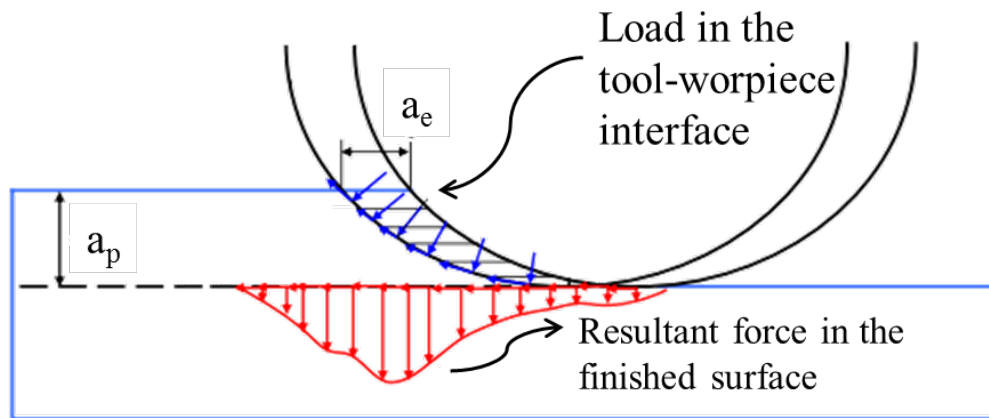
Figure 37 – Load in the tool-workpiece interface and resultant force in the finished surface (adapted from (GUILLEMOT, 2010)).

Considering that, for the end-milling modelling it was proposed that the loads shall be applied directly in the contact tool-workpiece zone. That generates the first hypothesis: only the cutting loads, applied in the contact zone, will represent the whole process, generating the real residual stress profile. Moreover, that approach will also interfere with the mesh size determination, because the dimensions of an element must to be small enough to represent the tool-workpiece contact when the tool passes by the point during the cutting.

Another consideration concerning the geometry of the model is the size of the workpiece that will be modelled. Two questions are observed to define that size:

- Maximum depth up to where RS are present;
- Mesh size.

The first point is more important than the second one. That is because, if the residual stress has its effects over deep regions of the workpiece, it will be mandatory to simulate that entire region to achieve the desired outcomes of the model. Jacobus, Devor and Kapoor demonstrate in their work (JACOBUS; DEVOR; KAPOOR, 2000) with annealed AISI 4340 that after 200 μm in-depth, negligible values of residual stresses were found. With that observation and also with the effects of the mechanical and thermal effect, they proposed a model for the residual stresses induced by the machining, as shown in Figure 38.
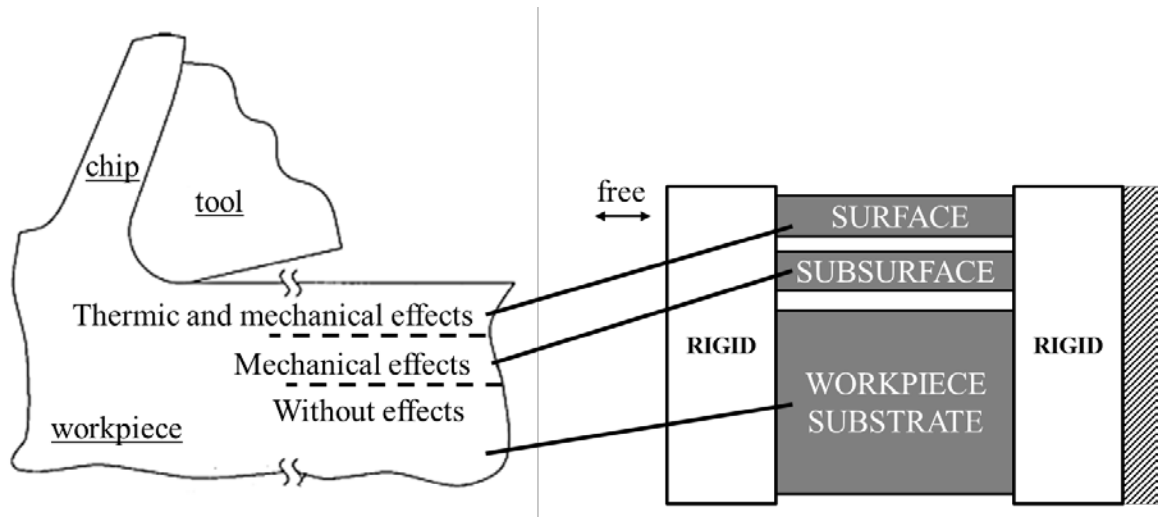
Figure 38 - Workpiece surfaces and their load effects (adaptaded from JACOBUS; DEVOR; KAPOOR, 2000).

Therefore, there exists a depth beyond which there are no more residual stresses generated by the mechanical and thermal loads. For that reason, the maximum depth that was simulated in this model is about 400 μm, as shown in Figure 39.
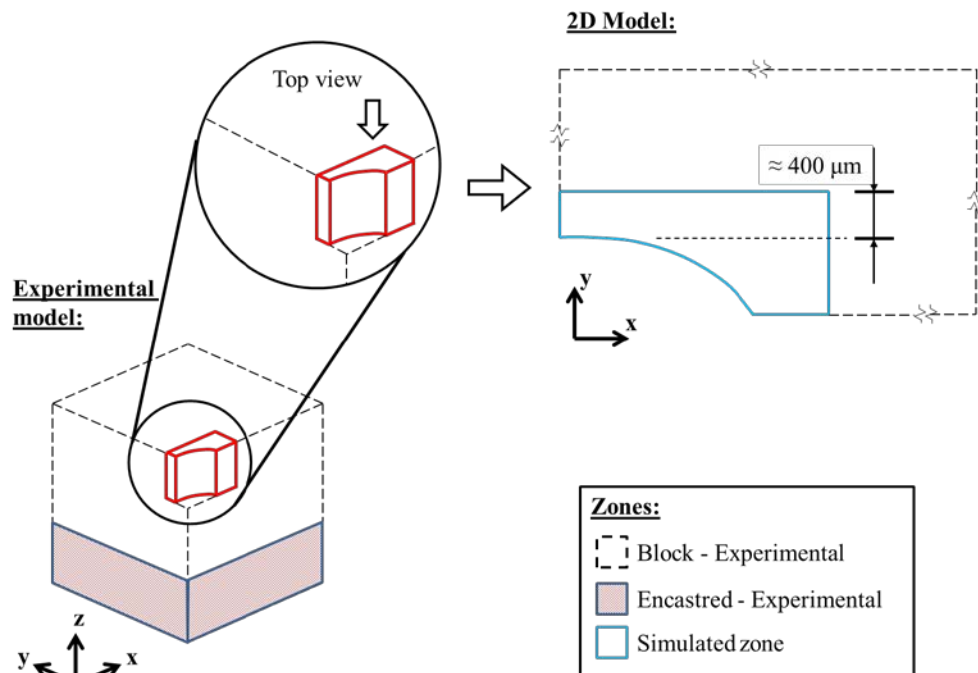
Figure 39 - Example of 3D model and 2D model with the zone simulated in the 2D model.

A detail must be considered: this depth value changes depending on the manufacturing process. So, if the hybrid method will be used to model another process, that value must be changed.

The last geometric assumption is related with the milling kinematic assumption and will be explained in the next section.

4.2.2. Kinematic assumption

Because of the relative movement that exists between the tool and the workpiece, with rotation and translation simultaneously on the tool, the real path that is described during the cut is a cycloidal. However, a simple assumption can be adopted: considering that, in the milling process of a large range of materials, the product of the tool radius and spindle speed is higher than the tool feed, the path can be considered as a circumference (SCHMITZ; SMITH, 2009). That assumption is completely related to the geometry, because the region for the load application (mechanical and thermal) will be circular and not cycloidal.

4.2.3. Material law assumption

For the material law, the classical assumptions that are already used for the workpiece material in a machining modelling were applied. Thus, the material that was simulated, besides the elastic behavior that is defined by the Young's modulus E and the Poisson's ratio v, has a thermo-visco-plastic behavior defined for Johnson-Cook equation 14. That mechanical law is used because the material, during a cutting operation, is submitted to high thermal, plastic deformation gradients, requiring a constitutive model that can considerer these parameters to achieve the desired outcomes.

For metals, the flow rule that was applied is associated.

4.2.4. Loading assumption

The loading assumptions will be the most important for this work because that will determine, in combination with the boundary conditions, if the model will be able to predict the residual stress field.

The first loading assumption was already considered in the section *Geometric assumption*, regarding the way how the loads will be applied. Instead of reducing the geometry to its final shape and applying the load only in the finished surface, the loads will be applied the cut is made, during the milling process.

Another assumption is related to the tool that will cut the workpiece. Depending on the milling tool in combination with the operation that will be executed, more than one contact may occur simultaneously, leading to different force profiles for the cutting. For that reason, this method is just proposed and tested with milling processes with the inexistence of simultaneous contact. Examples of different tool types are shown in Figure 40.

Figure 40 - Milling tools for different kinds of operations.

The understanding of the thermo-mechanical load behavior, during a cutting process, is one of the most important topics that must be known about the machining process. That importance is justified by the necessity to have a consistent force and temperature model to generate a coherent physical result of induced residual stresses.

4.2.5. Boundary condition assumption

The model must be a representation of the physical problem. However, with the geometric assumption, the model was reduced and, by consequence, part of the material was not included in the simulation. Thus, if a two-dimensional model is enough to express the residual stresses generated in a three-dimensional experimental model, then the boundary conditions will be equivalent. Otherwise, the finite element model will not correctly represent the milling process numerically and the result will not be physically coherent.

4.3. Definition of the finite element algorithm

In a classical model, where the tool-workpiece contact exists, the solution of the model is not possible to be obtained by the implicit solver. For that, the explicit solver is more

indicated to treat this kind of model. Its robustness is associated with the fact that it uses only the mass matrix in the computations instead of using the stiffness matrix as well (FONSECA, 2015).

Although the hybrid approach does not have contact in its model, the velocity that the load is applied suggests that the problem should be solved by the explicit algorithm. Moreover, the machining model has thermo-mechanical loads associated, which are solved in the ABAQUS® coupled only with explicit solver.

4.4. Definition of meshing

As mentioned in the section *Geometric assumption*, the way that the load will be defined will influence the meshing definition. As the tool moves during the milling operation, the loads will be applied at the node corresponding to the tool position. If a mesh is coarse, the distance between the points where the loads will be applied will also be large. A non-indicated and indicated example of mesh refinement is presented in Figure 41. So, the mesh must permit load application in a form similar that to is in a contact modelling.
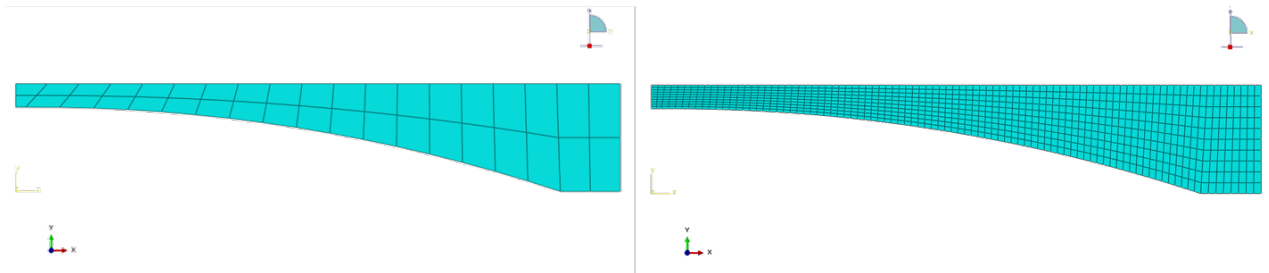
Figure 41 - Non-indicated mesh (left) and indicated mesh (right).

A second factor that will determine the mesh size is the residual stress gradient. It is observed that the residual stress induced by the machining process changes in a large range (changing from a tensile for a compressive behavior) in a narrow depth, varying from 50 μm to 100 μm. Therefore, if the mesh is coarse, the model will not be able to capture that gradient. For example, Valiorgue uses in his study an in-depth mesh size of 7.5 μm. So, in-depth meshing refinement should be used to represent that residual stress gradient (VALIORGUE, 2009).

The type of element that must to be selected needs to be able to support temperature-displacement solution. So, the CPE4RT (4-node bilinear displacement and temperature, with reduced integration with hourglass control) element type, which is a 4-node plane strain thermally coupled element, was selected.

The effects of the mesh size, according to the load representation and the residual stress obtained, was made, and it is presented in the chapter *Results and Discussion*.

4.5. Loading definition

To begin the loading definition and its representation in the model, the way that the load was obtained must to describe. In order to use this non-conventional method for other processes and, mainly, to use it in an industrial environmental, if this force-based approach is valid, the loads must be determined experimentally. According to the objectives described previously, the experimental procedures of this dissertation were based on the simulations to assess the use of the hybrid method, with the force-based approach, to model the residual stresses for milling. So, the experimental data that were used as the inputs to the model are provided by the dissertation of Maia (MAIA, 2015), that made the study of residual stresses generated by end-milling cutting in the titanium alloy Ti-6Al-4V. His research was developed in the laboratory CCM at ITA – São José dos Campos, being developed in the same period as the present approach to simulate the residual stresses.

The alloy that was used in his research is considered as a hard material to machine if compared to steel, being necessary to select cutting parameters such as type of milling process, type of tool material to resist the cutting forces and temperatures generated during the cutting (ZLATIN; FIELD, 1973).

The end-milling process was made in blocks of Ti-6Al-4V, with square base of 35 mm and 50 mm height. To execute the cut, a tool of diameter of 25 mm with two indexable inserts was used, being the forces generated during the process acquired by a piezoelectric platform placed in the base of the apparatus. The fixture system for the samples was specifically developed by Maia for this experimental procedure, in order to guarantee the rigidity for the fixation. The cutting was made with the axial depth (a_p) always equal 3 mm, with the variation of the radial depth (a_e), cutting speed (v_c) and feed (f_z). The temperature measurement was not made in his dissertation. The whole experimental set is shown in Figure 42.
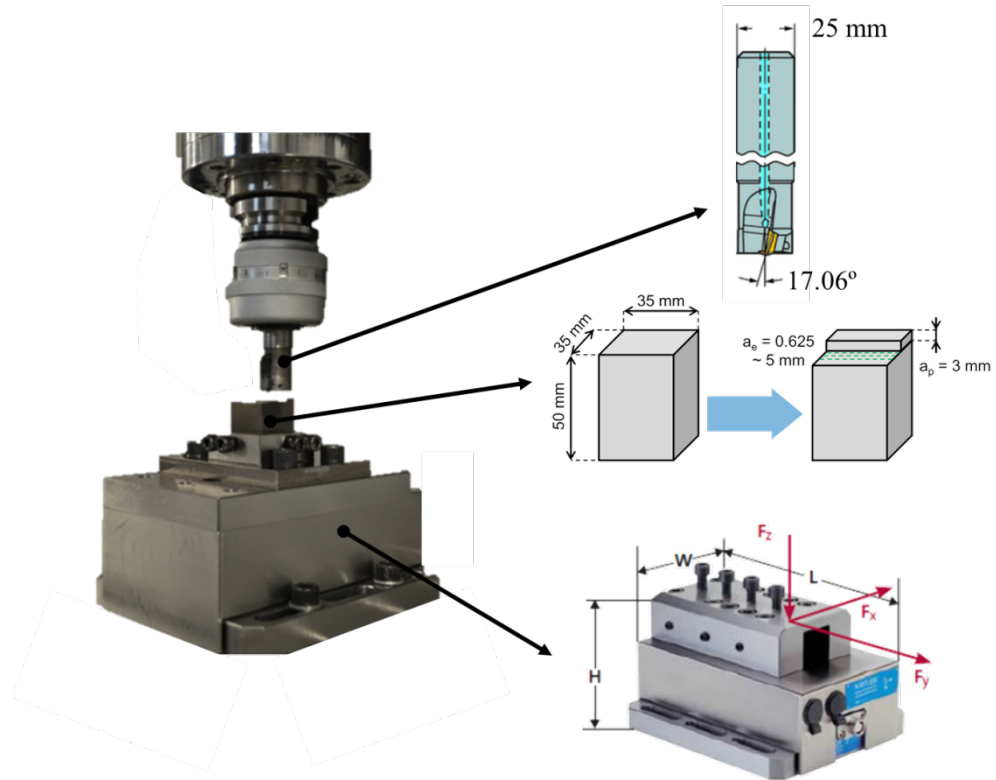
Figure 42 - Experimental set used by Maia (Adapted from MAIA, 2015).

The dynamometer was set to acquire the signal with a frequency of 4000 Hz. That frequency, as commented by Maia, is considered high because the tool pass in a frequency that varies in the range of 29.7 Hz to 38.2 Hz (MAIA, 2015). Three forces were measured: being F_x in the radial direction, F_y in the feed direction and F_z in the axial direction, as presented in Figure 42. Only the feed and axial force components were used because as observed by Maia, the axial component does not change the value of the cutting force F_c. Figure 43 shows the previous observation made by Maia.
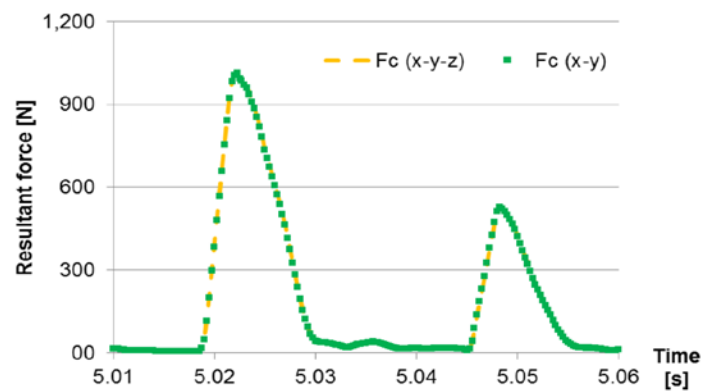
Figure 43 – Comparison of the cutting force considering and not the axial force component (MAIA, 2015).

Another factor that must be observed in the Maia's result is the variation of the force peaks, observed in Figure 43. He justifies the presence of those due to the runout which can be caused by the geometrical inaccuracy of the indexable tools. Therefore, to the first attempts for the hybrid simulation applied in the end-milling process, only the higher peak was considered. That assumption may induce a residual stresses in the modelling higher than the experimental data, because the effect of the residual stresses that the lower peak will cause will not be of the same magnitude.

The outputs of the dynamometer are force profiles in terms of time. The angular position of the tool is not directly known. Moreover, during the cutting of the 35 mm length, the inserts remove a large quantity of chips. Considering the acquisition frequency of 4000 Hz, the quantity of experimental points that was acquired is high and for the hybrid method, just one insert passage in the workpiece is necessary. For that reason, a data processing must be done before using the forces profiles, as shown in Figure 44.
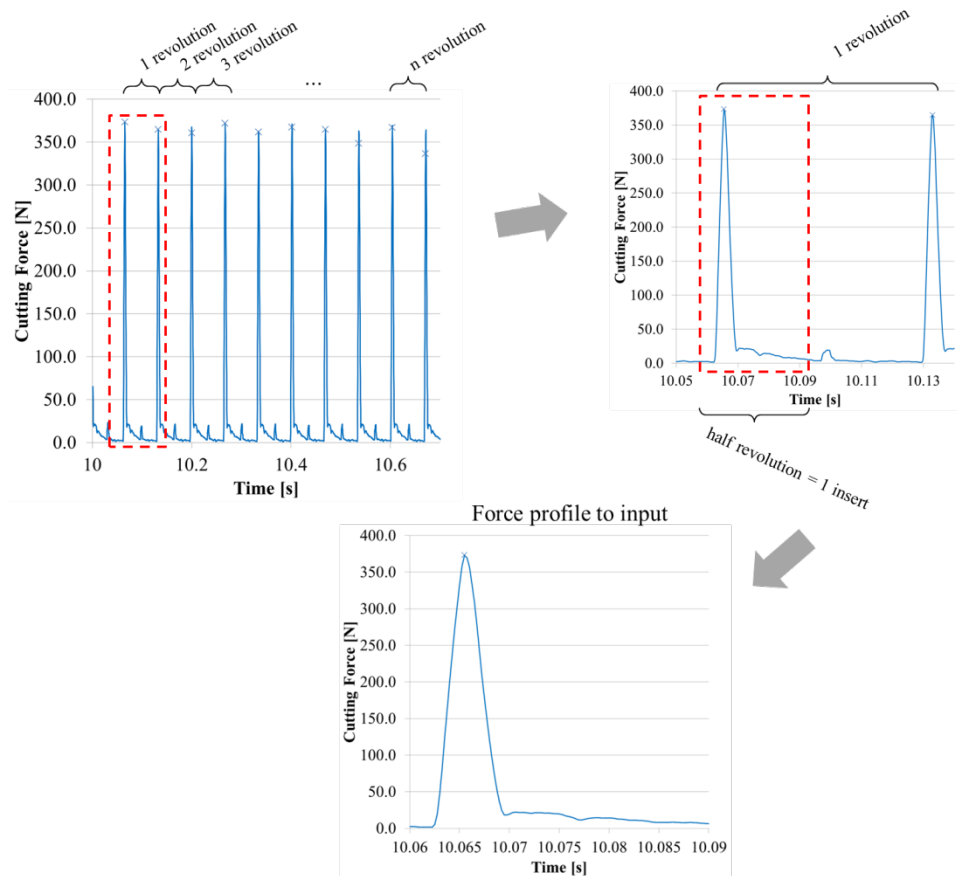
Figure 44 - Data treatment to select the force profile needed from Maia's results.

The treatment consists to find, in the force profiles, the data correspondent to the action of just one tool during one cut. The loads are applied in its components defined according to the cutting directions. Being the resultant force F_c a vector, its components can be defined in any reference system, as presented in Figure 45.
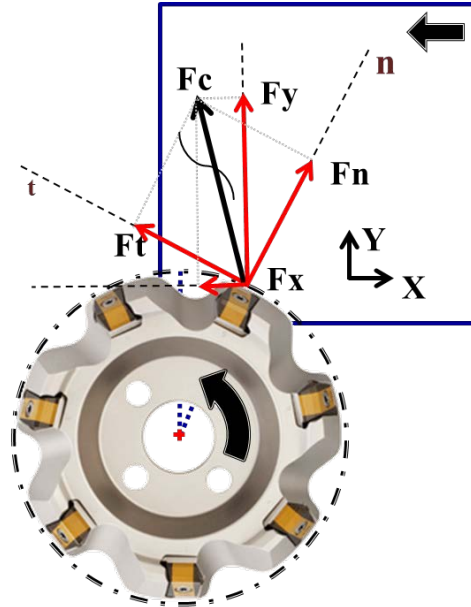
Figure 45 – Resulting force and its components at the application point.

If the reference system that is used in the dynamometer was different than the system used in the ABAQUS®, a rotation is necessary to apply the load with physical consistency. Nevertheless, the coordinate systems are coincident, leading to the application of the load without the necessity to rotate the system.

The application points must be consistent with the time when the force will be applied. Considering that the forces profiles that come from the experimental procedure are functions of time, an association to know the time t to a certain angular position must be made. The cutting angle described by the milling tool during the machining process is done by the equation 22 (DINIZ; MARCONDES; COPPINI, 2000).

$$\varphi_c = a\cos\left(1 - 2\frac{a_e}{D}\right) \tag{22}$$

Using the kinematic assumption once more, the time that the insert will require to cover that angle is:

$$t_c = \frac{60\varphi_c}{2\pi n} \qquad (23)$$

where n is the spindle speed, in RPM. If the number of nodes located at the cutting zone is known, the step time that will be between one node and the next is expressed as:

$$\Delta t = \frac{t_c}{n\_nodes} \qquad (24)$$

So, with the equation 24 the load as a function of time can be used directly. However, the meshing must be done beforehand and the kinematic assumption must be valid.

The nodes where the concentrated force is applied are selected one by one. However, this task, because of the meshing refinement is impossible to be done manually. An algorithm in MATLAB® was coded to execute that task. All the codes are presented in the Appendix. ABAQUS® writes, with all the modelling executed in its CAE module, an input file. That file is later read by the solver and contains the data needed to solve the problem. All the modifications that the MATLAB code made are in the input file, elimination the necessity to select nodes by hand. An example of that selection is shown in Figure 46. The nodes in green are generated by the ABAQUS® meshing module. The red nodes are the nodes analyzed to find the black node, where the loads are applied.
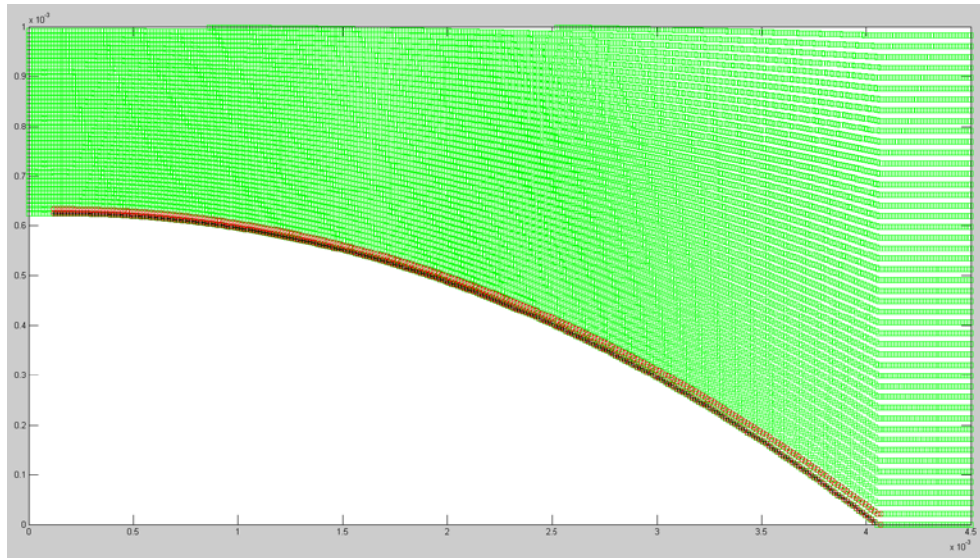

Figure 46 - Selected nodes in the node cloud.

The load that is in fact applied is divided into two parts: mechanical and thermal. The mechanical part is the load that is acquired by the experimental procedure. The thermal load is

defined as a function of the cutting power that is transformed in temperature during the cutting process, as was done by Valiorgue in his work. For the Ti-6Al-4V, the heat generated during the process is more dissipated in the tool, almost 75% (SCHROETER, WEINGAERTNER, 2002). So, a little percentage of the power will heat the titanium alloy, being considered as 10% to get the heat flux in the workpiece. All these loads are applied using the amplitude functions in ABAQUS. These functions are a way to define a load (independently of the type) as a function of time. Figure 47 presents the ramp type, used in this work.
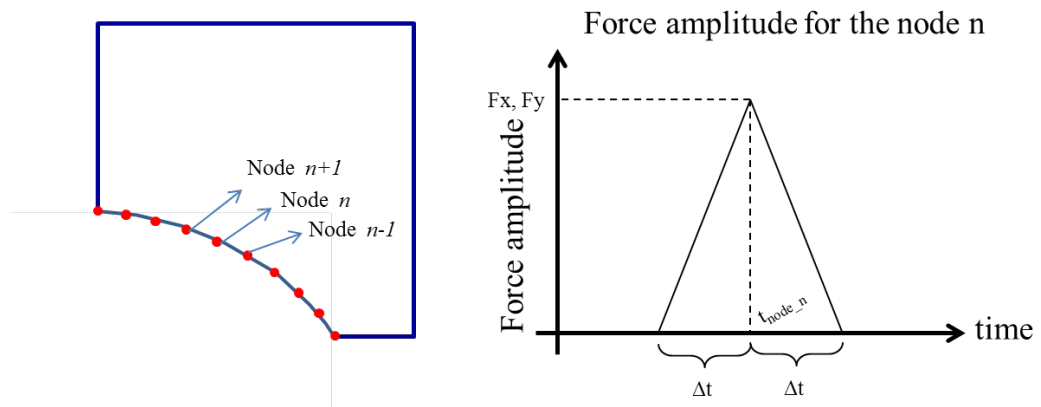
Figure 47 - Definition of force amplitude for a node *n* using the ramp amplitude function.

The whole simulation corresponds to one cutting time, that is, just one cut made by one tool. The quantity of cuts will depend of the process and the size of the workpiece that is cut. However, to understand the challenges with the milling simulation, just one passage of the tool was modelled. Locally at the nodes, the loads were defined with the help of the time step. In the time that was correspondent to the passage of the tool, the value of the force and thermal flux is the maximum. When the tool is between nodes *n-1* and *n* the loads increase their values from 0 to the maximum value in node *n*. After passing by the point, between the nodes *n* and *n+1* the loads decrease their values from the maximum value to 0. The same procedure is followed for all nodes that are located in the cutting zone. So, the load is discretized respecting the kinematic of the milling process without the presence of the tool.

4.6. Results expected

Concluding the idea of the residual stress simulation generated by the thermo-mechanical loads applied at the cutting zone using the hybrid method, the results that are expected are:

- Local plastification next to the representation of the tool passage in the workpiece, with its higher values in the beginning of the cut, since the end milling that was simulated is of the type of down milling;
- Residual stress field generated in the material due to the influence of the both loads applied;
- Temperature distribution with the higher temperature next to the end of the cutting.

5 Results and discussion

The fact that renders this proposal different from others is the load definition and where the load will be applied. The load is found by the association with the experimental cutting, measuring the cutting forces, with tribological experiment. Moreover, FEM is also used in interaction to find the friction coefficient and the heat partitioning fraction. These two parameters are related with the TSZ, where the mechanical load and the heat flux are applied. The pressure is found by Hertz theory, and that mechanical pressure is applied in the finished surface. The application that is modelled for the end-milling process is force-based, e.g., the forces that are measured in the experimental procedure are directly applied at the cutting zone, in accordance with the kinematic of the process. The heat flux is calculated as a function of the cutting forces and is applied in the same model.

Figure 48 presents, in the left-hand side, the application of the cutting force at some moment, during the cut. The right-hand side, the figure on the top presents the classic model and its application whereas the figure on the bottom present the hybrid method developed by Valiorgue.
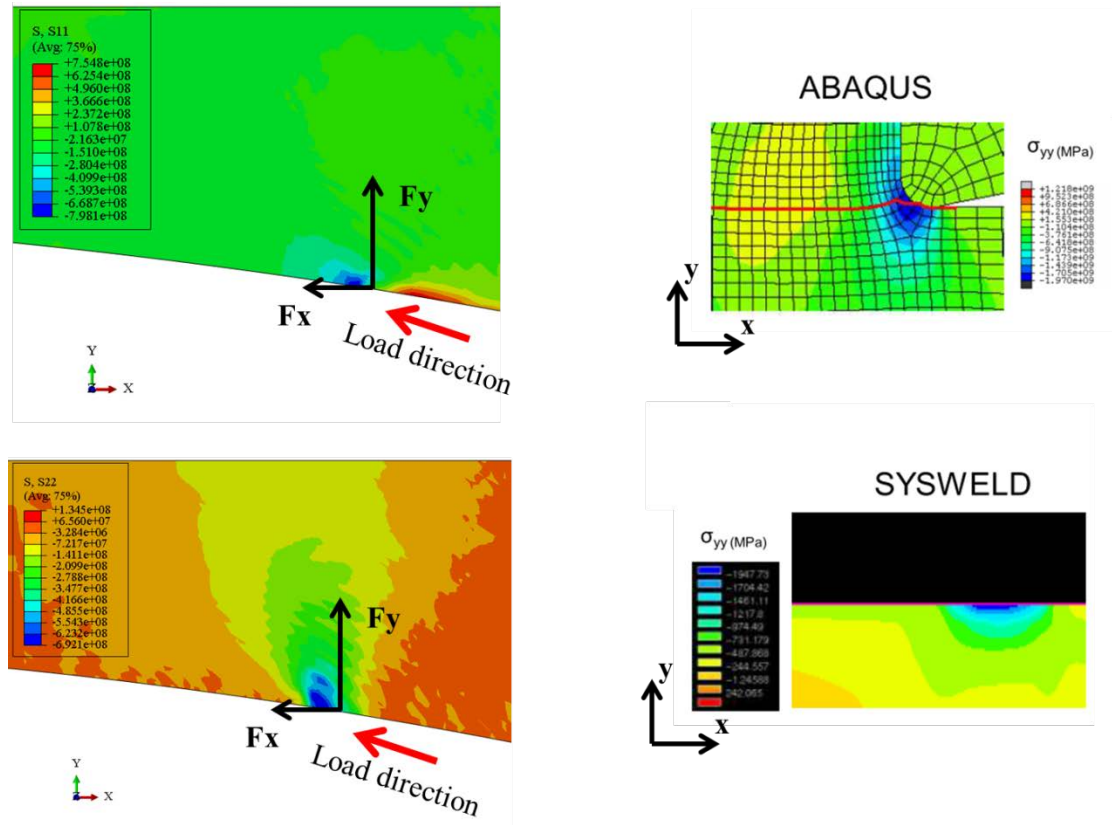
Figure 48 - Equivalence among the load application (adapted from (VALIORGUE, 2009)).

Even though the cutting directions are not the same two points are worth mentioning:

a) The two figures in the right-hand side present a compressive zone in front of the tool/ cutting zone and a tractive zone behind the tool/cutting zone;

b) In the left-hand size, with the association of the x-normal stress field and y-normal stress field, it is possible to conclude that there exist a compressive zone in front of the tool and a tractive zone behind the tool.

These two points permit to conclude that, although not expressing the same stress field, quantitatively speaking, due to the difference in the cutting condition and the material that constitute the workpiece, the characteristics of the fields that are observed are similar. The compression zone that is visualized in front of the tool is physically observed. That fact can express evidence that the cutting forces, applied directly in the nodes respecting the machining kinematic, as a concentrated force, could be used to express a milling process.

Another equivalence that exists is related to the temperature distribution. Comparing with Guillemot's work (GUILLEMOT, 2010) it is possible to see in Figure 49 the similarity between the temperature distribution.
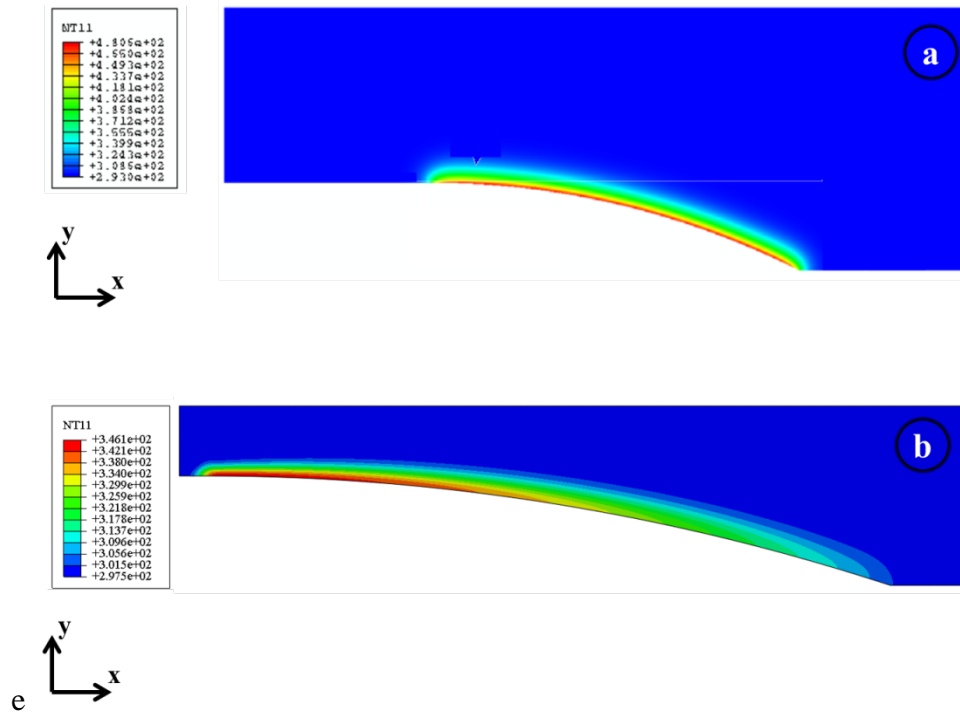
Figure 49 - Heat distribution after cut: a) ball-nose milling process (GUILLEMOT, 2010); b) end-milling process.

The heat distribution presented in Figure 49a is different from the other one due to the process. The reason is how the heat flux was applied in the two models. In the first, the tool axis is oblique to the XY-plane, as indicated in Figure 50.
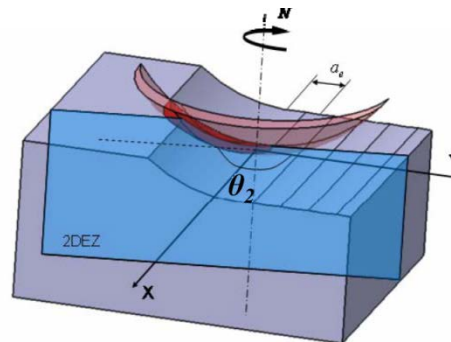
Figure 50 - Angle between the tool axis and the XY-plane (GUILLEMOT, 2010).

The contact between the tool-workpiece will not be considered as concentrated in a specific region, being distributed in all the arc of the contact. The end-milling process has the tool axis perpendicular to the plane. Thus, the contact between tool-workpiece is localized in a concentrated zone. With the evolution of the cut, the heat that was generated in the beginning of the cut was transmitted to the workpiece, increasing the internal temperature.

Therefore, at the end of the cut of one chip, a non-uniform heat distribution can be observed in the end-milling cutting. The same condition cannot be observed in the turning case, because the cut is continuous and, for that, the heat flux will be applied at every moment, as shown in Figure 51.
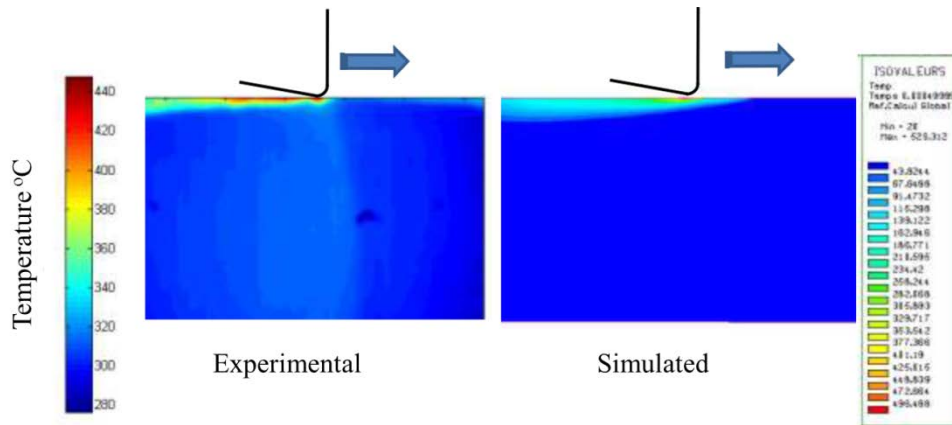
Figure 51 - Experimental and simulated temperature distribution after a turning process (VALIORGUE, 2009).

The force being applied is presented in Figure 52.
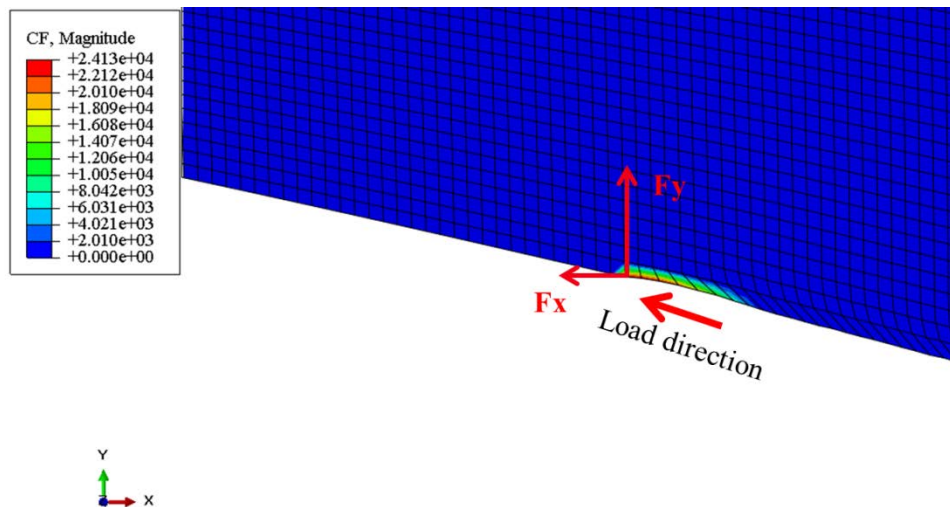
Figure 52 - Load application example.

If the force is high enough to promote the plastification in the material, that plasticity zone, and also the stress redistribution, will result in a residual stress field. Focusing in the machining processes, that force will cause shearing of the material. Also, its effects will heat up the material in the shear zone by the plastic deformation and the friction between the tool and workpiece in the tertiary shear zone. Therefore, if a residual stress prediction with the

forces and heat flux as input data will be representative of the machining process, these loads must generate:

- Local plastification next to the cutting zone;
- Rise in temperature next to the cutting zone.

First, a representative constitutive data for the model was searched. The Johnson-Cook model, as presented in the *Literature Review*, was used in the model. The values for the constants are presented in Table 4.

Table 4 - Johnson-Cook parameters ($\dot{\varepsilon}$ = 2000 1/s) (RAO; DANDEKAR; SHIN, 2011)

Johnson-Cook parameters						
A (MPa)	B (MPa)	C	n	m	Tm (K)	Tf (K)
883.9	598.8	0.0335	0.361	1.041	1933	296

Rao, Dandekar and Shin (RAO; DANDEKAR; SHIN, 2011), in their work made a comparison of the JC parameters, for Ti-6Al-4V alloy, to test what was more characteristic for the force prediction. The data set that is presented in Table 4 is, among the data sets that were studied, one of the most representatives. For that reason, it was selected for this work. The other physical properties that were used are presented in Table 5.

Table 5 - Ti-6Al-4V physical properties (LEYENS; PETERS, 2003)

Ti-6Al-4V physical parameters				
E (GPa)	v	K (W/m k)	cp (J/ kg K)	ρ (kg/m³)
114	0.34	3.069	564	4430

The thermal convection was modelled with the external environment. The heat transfer coefficient used was 46 W/m² (VALIORGUE, 2009). The external media was considered at a temperature of 25 ºC.

When it comes to the temperature aspect, the milling of the Ti-6Al-4V alloy was simulated with the experimental cutting condition executed by Maia in his master's dissertation (MAIA, 2015). The cutting condition can be considered as soft, because the radial depth of cut (a_e) was not high. The value of the feed per tooth was, among the used values, the highest. However, in combination with the radial cut, the force generated was not considerable. Table 6 presents the 16 conditions tested at a flood cut condition, with the cutting force used selected.

Table 6 - Mean force values, in Newtons, for each tested machining condition (MAIA, 2015).

v_c = 70 m/min		f_z [mm/tooth]			
		0.075	0.100	0.125	0.150
	0.625	354	402	451	496
a_e	1.250	452	532	594	626
[mm]	2.500	589	670	764	817
	5.000	683	834	932	1012

The criterion to select this cutting condition was the chip size, which was the smallest among all the tested conditions. The force profiles related to this cutting condition are presented in Figure 53.
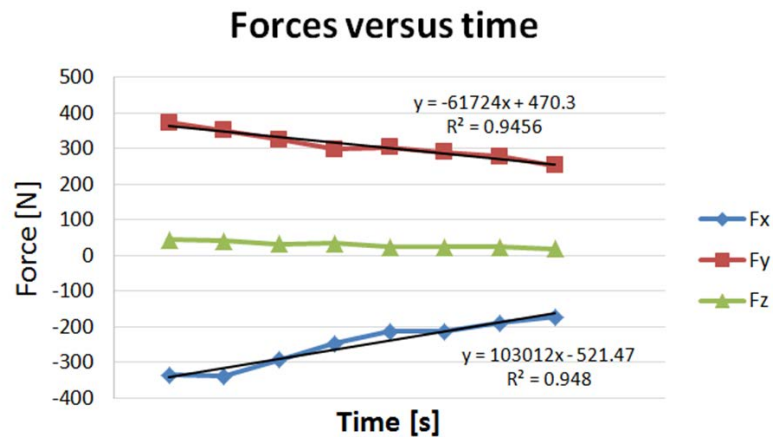
Figure 53 - Force profiles related with the cutting condition selected from Maia's results.

The values of the R² are almost 0.95 for the forces along the two directions and represent a good fits of the linear curves with the experimental data. With that regression, and the support of the algorithm presented in the *Appendix*, the distribution of the cutting load is possible, resulting in the model presented in Figure 54.
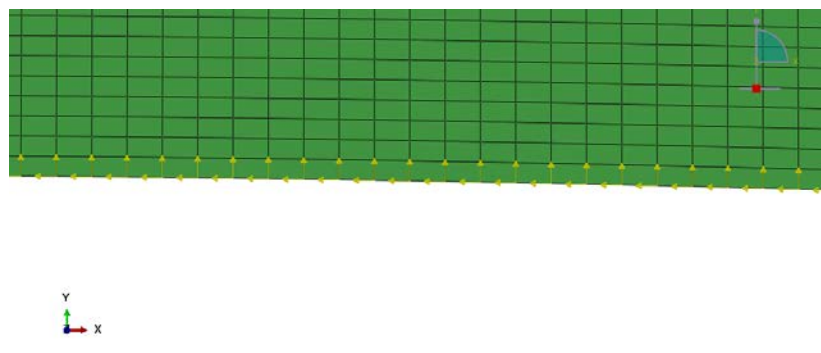
Figure 54 - Nodal concentrated force.

The results, in terms of plastic deformation and temperature are shown in Figure 55 and Figure 56.
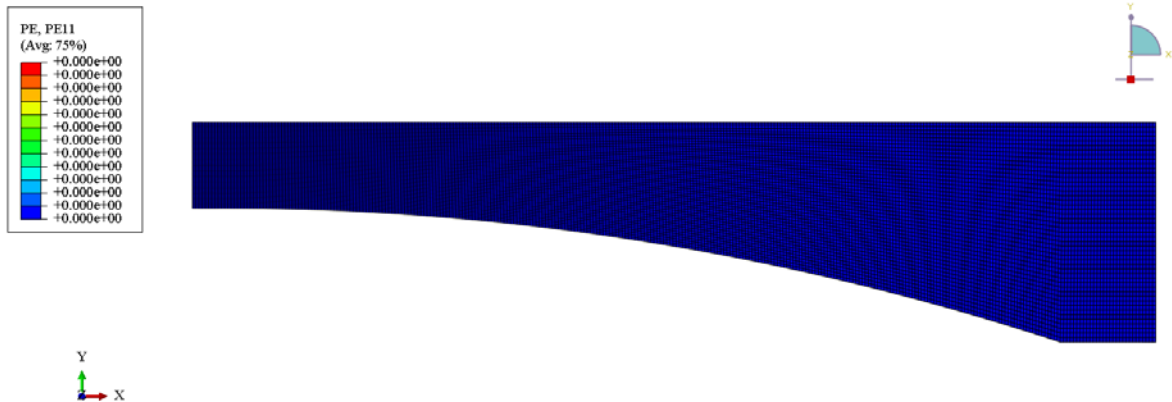
Figure 55 - Plastic deformation after one cut.
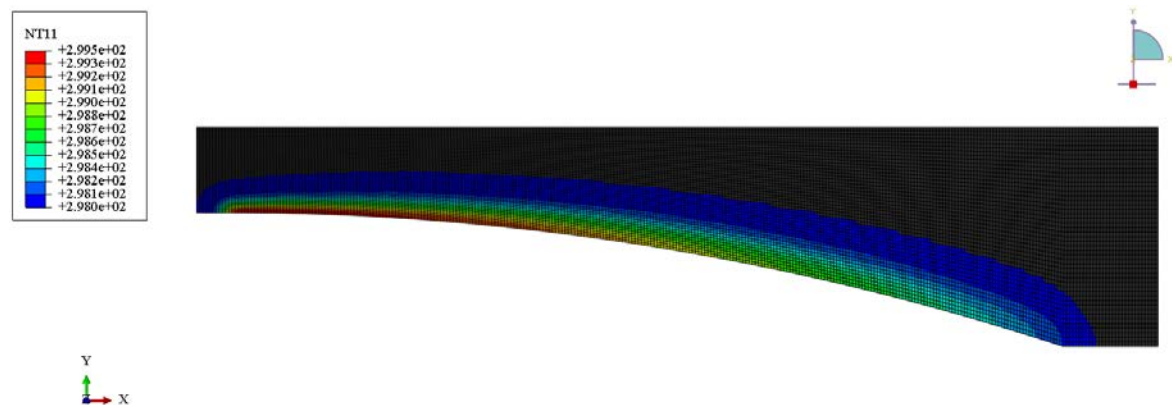
Figure 56 - Thermal distribution after one cut.

As observed, the loads did not generate the plastification leading to an erroneous conclusion that the forces that are measured are not enough to generate residual stresses. However, these forces are measured in a cutting process, where they promoted the cutting of the material. So, their effects are enough to cut the material and generate local plastification.

As a 2D model, the thickness that is associated with the geometric model, to simulate a solid behavior must to be provided, as indicated in Figure 57.
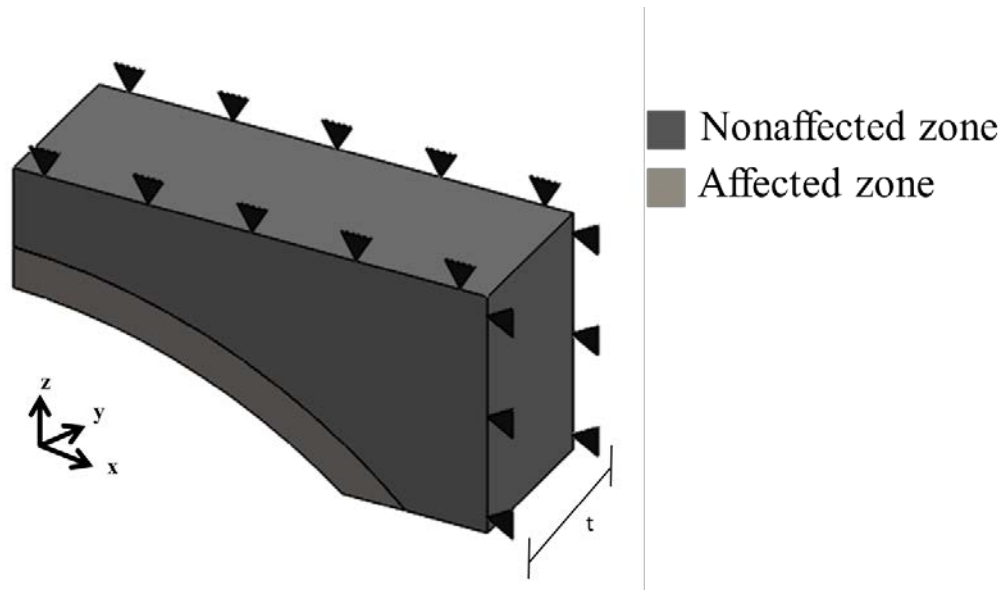
Figure 57 - Thickness association to a 2D model.

Although not visualized during the modelling step, that thickness will be considered in the solver step. The same as in a beam submitted to a bending load, in Timoshenko beam theory. Even the modeling of the cross section was not made in the geometry, it must to be provided, because the section properties are considered in the formulation. Therefore, a plane stress-strain thickness must be provided.

Considering the cutting process that was modelled with the hybrid method, the radial depth of the process equals 3 mm. This is the value of the plane stress-strain thickness used. The results associated with that thickness are presented in the Figure 58 and Figure 59.

Figure 58 - Plastic deformation associated with a plane stress-strain thickness of 3 mm.
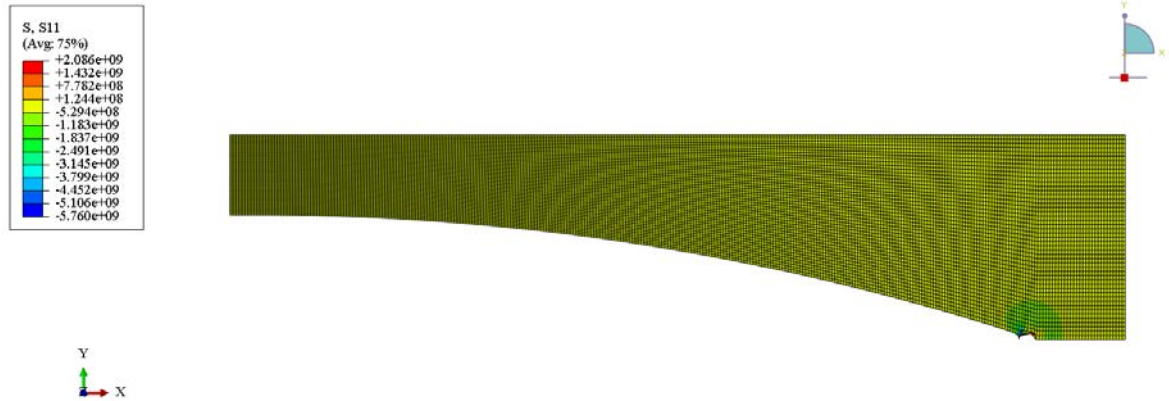
Figure 59 – X-normal residual stress associated with a plane stress-strain thickness of 3 mm.

Again, even with a plane stress-strain thickness equivalent to the cutting condition, the results obtained are not physically coherent. In this case, instead of having absolutely no effects of the loads, a high local plastic deformation was found. These results are leading to another false conclusion about the loads that are measured in the process, because their effects are not large enough to produce a local deformation as the one reported in Figure 58.

Now, considering the value of that thickness equal to 30 mm, which is equivalent with the dimension of the whole block that was used in the experimental procedure, the results presented in Figure 60, Figure 61 and Figure 62 were found.
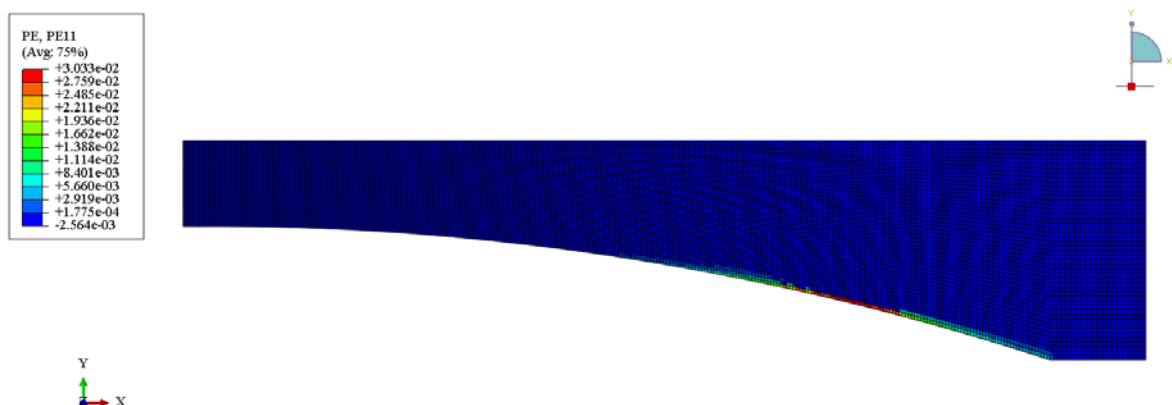
Figure 60 - Plastic deformation associated with a plane stress-strain thickness of 30 mm.
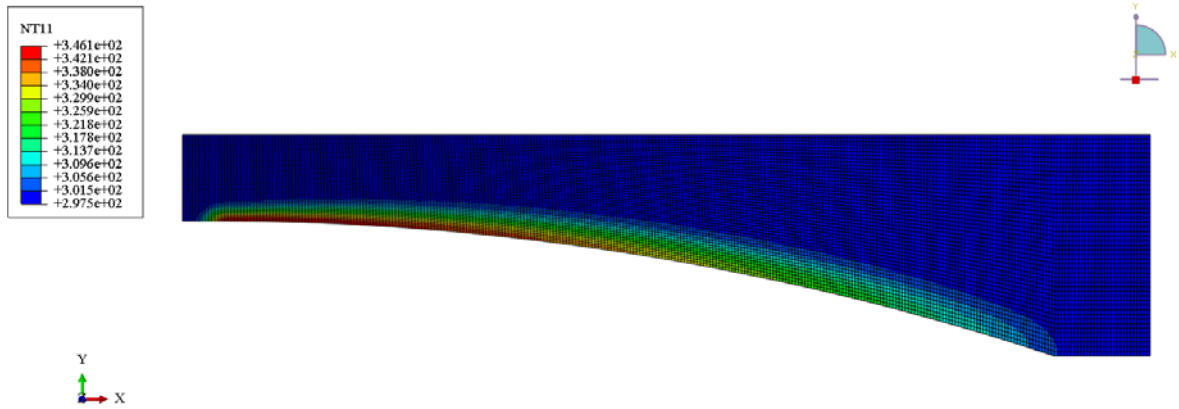
Figure 61 – Thermal distribution associated with a plane stress-strain thickness of 30 mm.
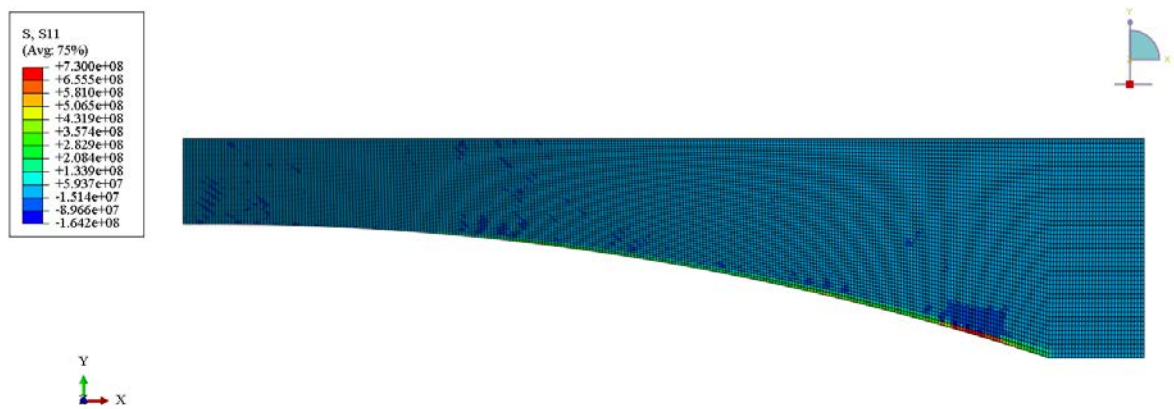
Figure 62 - X-normal residual stress associated with a plane stress-strain thickness of 30 mm.

The results observed in Figure 60, Figure 61 and Figure 62 are more reasonable and realistic. Plastic deformation, increase in temperature and, therefore, the origin of residual stresses were observed. The experimental dataset reported by Maia (2015) in his dissertation has, for that cutting condition, the residual stress in the surface of -260.1 MPa ±25.7 MPa. If a region corresponding to the finished surface was analyzed, in the simulated model, the residual stress that is found is -164.2 MPa. The error between the experimental and simulated results is about 30%.

A discussion about the effect of the plane stress-strain thickness must be made to understand the discrepancy. First of all, even with 3 mm and 30 mm, the effects of the loads in the workpiece were wrong, physically speaking. With the correlation of the thickness with the cutting variables, the plane stress-strain thickness is equals the axial depth. So, it was expected for the value of 3 mm comparable outcomes (experimental and numerical). However, a numerical results that was compared with the experimental data, was associated

with a 30 mm thickness, which is not true. The chip that was generated during the process is 3 mm of height whereas, according the dimensions that was used in the model, that value was 30 mm. The energy provided by the load (experimentally acquired), to generate the residual stress equivalent with the experimental measures, corresponds to a 30 mm height chip.

The consequence of the fixing procedure that was applied when the block was tested and its representation in a two-dimensional model, as shown in Figure 39, may explain that model misbehavior. Even though the forces measured are associated with the form that the block was fixed, the effect of these loads in the surface that was machined is local. That is, the plastic effects, thermal generation and, therefore, the generation of residual stress, are localized next to the cutting zone, regardless of the experimental boundary conditions. These local effects are in accordance with several studies with residual stresses generated by machining measurements. Moreover, the model proposed by Jacobus, DeVor and Kappor (JACOBUS; DEVOR; KAPOOR, 2000), presented in Figure 38 goes in the same direction. Therefore, in terms of force, the simplification between the two-dimensional and three-dimensional model may not be possible.

When the work of Valiorgue (VALIORGUE, 2009) is perused observed, the definition of the model in terms of pressure can be seen as an option to avoid the problem with the thickness, because it will be considered in the pressure definition. However, considering the contact between tool-workpiece at the TSZ, the alteration in the thickness must be followed by and alteration in the force magnitude to maintain the pressure value. Thus, both methods to apply the hybrid approach (pressure-based, done by Valiorgue and force-based, proposed in the dissertation) have its considerations about the load application.

6 Conclusions and suggestions for future developments

In accordance with other methods that are applied to predict residual stresses, generated by machining process, the hybrid approach considering the force as a direct input was considered possible, due to its equivalence with the compressive-tensile zones and the relationship between them and the cutting direction. Moreover, the temperature distribution supports that observation, with a reasonable equivalence between the thermal distribution found in the literature and in the simulation.

As it was discussed, the force-based hybrid approach to the milling process has a sensibility related to the plane stress-strain thickness, when a 2D model is done. A misbehavior that was observed is indicative that, even with the reasonable stress fields obtained during the machining process, the effects caused by the load are not well described. A solution for that problem is the application of the pressure-based model, as proposed by Valiorgue in his doctorate thesis.

In accordance with the previous point, a solution that can be proposed is the use of the same method, however in a 3D model, considering the boundary conditions as the same as the fixation method used in the experimental procedure, guaranteeing the maximum equivalence among experimental and simulation.

References

ARRAZOLA, P. J. *et al*. Recent advances in modelling of metal machining processes. **CIRP Annals-Manufacturing Technology**, v. 62, n. 2, p. 695-718, 2013.

ARRAZOLA, P. J. *et al*. Investigations on the effects of friction modeling in finite element simulation of machining. **International Journal of Mechanical Sciences**, v. 52, n. 1, p. 31-42, 2010.

ASTAKHOV, V P. Surface integrity–definition and importance in functional performance. In: DAVIM, J. P. (Ed.). **Surface Integrity in Machining**. New York: Springer London, 2010. p. 1-35.

BATHE, K.-J. **Finite element procedures in engineering analysis**. Prentice Hall, 1982.

BHADESHIA, H. K. D. H., Material factors. In: **Handbook of Residual Stress and Deformation of Steel.** Materials Park: ASM. p. 3-10, 2002.

BUDAK, E. Analytical models for high performance milling. Part I: Cutting forces, structural deformations and tolerance integrity. **International Journal of Machine Tools and Manufacture**, v. 46, n. 12, p. 1478-1488, 2006.

CALAMAZ, M; COUPARD, D; GIROT, F. A new material model for 2D numerical simulation of serrated chip formation when machining titanium alloy Ti–6Al–4V. **International Journal of Machine Tools and Manufacture**, v. 48, n. 3, p. 275-288, 2008.

CERETTI, E. *et al*. Turning simulations using a three-dimensional FEM code. **Journal of Materials Processing Technology**, v. 98, n. 1, p. 99-103, 2000.

CRISFIELD, M. A. **Non linear finite element analysis of solids and structures**, v. 1 and 2. Willey, 1997.

DINIZ, A. E.; COPPINI, N; MARCONDES, F. C. **Tecnologia da usinagem dos materiais**. São Paulo: Art Liber Editora, p. 244, 2000.

DASSAULT SYSTÈMES. **ABAQUS® CAE User's Manual, Version 6.11**. [S.l.: s.n.], 2011

DEUTSCHES INSTITUT FÜR NORMUNG. **DIN 8580:2003-09** Fertigungsverfahen Begriffe, Einteilung. Berlin, 2003.

FONSECA, Luiz Guilherme Aun. **Crankshaft deep rolling modeling through explicit analysis using finite element method.** 2015. 108f. Dissertation of Master of Science in Aeronautics and Mechanical – Instituto Tecnológico de Aeronáutica, São José dos Campos.

FUNATANI, K. Residual stresses during gear manufacture. **Handbook of Residual Stress and Deformation of Steel**, Materials Park: ASM p. 437-458, 2002.

GOMES, Jefferson de Oliveira. **Análise da usinabilidade de aços inoxidáveis austeníticos SAE 304 e SAE 316 com a variação dos parâmetros metalúrgicos**. 1996. 105f. Tese de Doutorado. Universidade Federal de Santa Catarina, Florianópolis.

GUILLEMOT, Nicolas. **Prise en compte de l'intégrité de surface pour la prévision de la tenue en fatigue de pièces usinées en fraisage**. 2010. 259f. Tese de Doutorado. École normale supérieure de Cachan-ENS, Cachan.

GUILLEMOT, N. *et al*. 3D heat transfer analysis for a hybrid approach to predict residual stresses after ball-end milling. **Procedia Engineering**, v. 19, p. 125-131, 2011.

GUPTA, K *et al*. Recent developments in sustainable manufacturing of gears: a review. **Journal of Cleaner Production**, v. 112, p. 3320-3330, 2016.

HUTTON, D. **Fundamentals of finite element analysis**. McGraw-Hil,, 2004.

JACOBUS, K; DEVOR, R. E.; KAPOOR, S. G. Machining-induced residual stress: experimentation and modeling. **Journal of Manufacturing Science and Engineering**, v. 122, n. 1, p. 20-31, 2000.

JASPERS, S. P. F. C.; DAUTZENBERG, J. H. Material behaviour in metal cutting: strains, strain rates and temperatures in chip formation. **Journal of materials processing technology**, v. 121, n. 1, p. 123-135, 2002.

JAVIDI, Ataollah. **Influence of Machining on the Surface Integrity and Fatigue Strength of 34CrNiMo6 Steel**. 2008. 147f. Doctorate Thesis - The University of Leoben, Leoben.

JOHNSON, G. R.; COOK, W H. A constitutive model and data for metals subjected to large strains, high strain rates and high temperatures. In: **Proceedings of the 7th International Symposium on Ballistics**. 1983. p. 541-547.

KLOCKE, F. **Manufacturing processes 1:** cutting**.** 1st ed. Berlin: Springer, 2011. 504p**.**

LEYENS, C.; PETERS, M. (Ed.). **Titanium and titanium alloys**. 1st ed. Wiley-VCH, Weinheim, 2003, 503p

LÖHE, D.; LANG, K.-H.; VÖHRINGE, O. Residual stresses and fatigue behavior. In: **Handbook of Residual Stress and Deformation of Steel.** Materials Park: ASM. p. 27-53, 2002.

LU, J. Prestress engineering of structural material: a global design approach to the residual stress problem. **Handbook of Residual Stress and Deformation of Steel**, Materials Park: ASM p. 11-26, 2002.

MAIA, André Hemerly. **Impacts on the surface integrity of titanium milling with minimum quantity lubrication and flood of coolant**. 2015. 118f. Dissertation of Master of Science in Manufacturing Technology – Instituto Tecnológico de Aeronáutica, São José dos Campos.

MAUREL, A. *et al*. Experiments and FEM simulations of milling performed to identify material parameters. **International Journal of Material Forming**, v. 1, n. 1, p. 1435-1438, 2008.

MOVAHHEDY, Mohammad R. **ALE simulation of chip formation in orthogonal metal cutting process**. 2000. Tese de Doutorado. University of British Columbia.

MUÑOZ-SÁNCHEZ, A. *et al*. Numerical analysis of the tool wear effect in the machining induced residual stresses. **Simulation Modelling Practice and Theory**, v. 19, n. 2, p. 872-886, 2011.

ÖZEL, T.. The influence of friction models on finite element simulations of machining. **International Journal of Machine Tools and Manufacture**, v. 46, n. 5, p. 518-530, 2006.

RAO, B; DANDEKAR, C R.; SHIN, Y C. An experimental and numerical study on the face milling of Ti–6Al–4V alloy: Tool performance and surface integrity. **Journal of Materials Processing Technology**, v. 211, n. 2, p. 294-304, 2011.

RAO, S. S. **The Finite Element Method in Engineering**. 4th ed. Elsevier Science & Technology Books, 2004.

REGO, R. R. **Influência do uso de distribuição bimodal de classes de granalha no processo de shot peening sobre o perfil de tensões residuais de engrenagens**. 2011. 183f. Dissertação de Mestrado. Faculdade de tecnologia SENAI CIMATEC, Salvador.

RECH, J.; CLAUDIN, C.; D'ERAMO, E. Identification of a friction model—application to the context of dry cutting of an AISI 1045 annealed steel with a TiN-coated carbide tool. **Tribology International**, v. 42, n. 5, p. 738-744, 2009.

SCHMITZ, T L.; SMITH, K. S. **Machining dynamics**: frequency response to improved productivity. Springer Science & Business Media, 2008.

SCHROETER, R. B.; WEINGAERTNER, W. L. **Tecnologia da usinagem com ferramentas de corte de geometria definida–parte 1**. 2002.

SHET, C; DENG, X. Finite element analysis of the orthogonal metal cutting process. **Journal of Materials Processing Technology**, v. 105, n. 1, p. 95-109, 2000.

SOO, S. L.; ASPINWALL, D. K.; DEWES, R. C. 3D FE modelling of the cutting of Inconel 718. **Journal of Materials Processing Technology**, v. 150, n. 1, p. 116-123, 2004.

SORIANO, H. L.; LIMA, SILVIO DE SOUZA. **Método de Elementos Finitos em Análise de Estruturas**. EdUSP, 2003.

SOUZA, Milena Chanes de. **Avaliação das dimensões técnico/econômica, ambiental e social no fresamento com aplicação de distinstas técnicas de lubri-refrigeração**. 2014. 167f. Dissertação de mestrado em Materiais e Processos de Fabricação – Instituto Tecnológico de Aeronáutica, São José dos Campos.

STYGER, G; LAUBSCHER, R. F.; OOSTHUIZEN, G. A. Effect of constitutive modeling during finite element analysis of machining-induced residual stresses in Ti6Al4V. **Procedia CIRP**, v. 13, p. 294-301, 2014.

TLUSTY, J. **Manufacturing processes and equipment**. Prentice Hall, 2000.

VALIORGUE, F. *et al*. A new approach for the modelling of residual stresses induced by turning of 316L. **Journal of materials processing technology**, v. 191, n. 1, p. 270-273, 2007.

VALIORGUE, Frédéric. **Simulation des processus de génération de contraintes résiduelles en tournage du 316L Nouvelle approche numérique et expérimentale**. 2009. Tese de Doutorado. Université Paris VI.

ZEMZEMI, F. *et al*. Identification of a friction model at tool/chip/workpiece interfaces in dry machining of AISI4142 treated steels. **Journal of materials processing technology**, v. 209, n. 8, p. 3978-3990, 2009.

ZLATIN, Norman; FIELD, Michael. Procedures and precautions in machining titanium alloys. In: **Titanium science and technology**. Springer US, 1973. p. 489-504.

Appendix

The codes that are used to identify the nodes and made the corrections on the Abaqus input file are presented below.

```matlab
% Esse código é destinado ao auxílio na modificação do arquivo de input
% para a simulação do Abaqus, colocando os nós nos quais são aplicados os
% carregamentos em ordem.
% Versão 4.2 capaz de definir carregamento termomecânico

clear all
close all
clc

%% Cálculo dos tempos de aplicação para cada função de amplitude
fprintf('-- VARIÁVEIS DE CORTE -- \n');

n_tools=input('O fresamento é feito com quantos insertos/facas? ');
tool_d=input('Qual é o diâmetro da ferramenta de corte [mm]? ');
ae=input('Qual o valor da profundidade de corte [mm]? ');
fz=input('Qual o valor do avanço por dente [mm]? ');
RPM=input('Qual a velocidade de rotação do spindle [RPM]? ');

cutting_angle=acos(1-2*(ae/tool_d)); % Ângulo de corte, em radianos
cutting_time=60*cutting_angle/(2*pi*RPM); %Tempo de corte, em segundo
relaxation_time=((60/RPM)-n_tools*cutting_time)/n_tools;

%% Entrada do número de cavacos e quantidade de pontos por cavaco
fprintf('\n\n-- DETALHES GEOMÉTRICOS DO MODELO -- \n');
length=input('Informe o comprimento do retângulo para simulação [mm]: ');
width=input('Informe a largura do retângulo de simulação [mm]: ');
n_chip=input('Quantos cavacos serão simulados? ');

%% Entrada dos números dos pontos nodais
```

```matlab
fprintf('\n\n-- DETALHES DA MALHA: NECESSÁRIO SABER A NUMERAÇÃO DO
PRIMEIRO NÓ DO PRIMEIRO CAVACO -- \n');
seed=input('Informe o tamanho do seed [mm]: ');


[node_chip]=id_nodev20(tool_d,ae,fz,length,width,n_chip,seed,cutting_angle);


nodes=node_chip;
n_points=size(node_chip,2); %Quantidade de nós para cada cavaco


%% Cálculo das forças Fx e Fy para cada ponto
fprintf('\n\n                    -- MODELO DE CARREGAMENTO: NECESSÁRIO
ALGUM MODELO DE FORÇA E POTÊNCIA DE CORTE NA FORMA POLINOMIAL
(MESMA ORDEM PARA OS MODELOS) -- \n');


degree=input('Qual o grau do polinômio que representa seu modelo de carregamento? ');
load_coef=zeros(3,degree+1);


part_time=zeros(1,n_points); %Criação de uma matriz linha com a quantidade de pontos
iguais ao número de nós/cavaco
step_time=cutting_time/n_points;


for i=1:n_points-1
    part_time(1,i+1)=part_time(1,i)+step_time;
end


for i=1:3


    switch i
        case 1
            fprintf('\nPara os esforços da direção x, em Newtons, diga:\n');
        case 2
            fprintf('\nPara os esforços da direção y, em Newtons, diga:\n');
        case 3
            fprintf('\nPara a potência de corte, em Watts, diga:\n');
```

```matlab
        otherwise
    end


    for j=1:degree+1
        fprintf('Qual o coeficiente para o termo de grau %u:',j-1)
        load_coef(i,j)=input(' ');
    end

end

load=zeros(3,n_points); %Matriz de força preparado para as direções x e y apenas

for i=1:degree+1

    for j=1:n_points
        load(1,j)=load(1,j)+load_coef(1,i)*part_time(1,j)^(i-1); %Força X
        load(2,j)=load(2,j)+load_coef(2,i)*part_time(1,j)^(i-1); %Força Y
        load(3,j)=load(3,j)+load_coef(3,i)*part_time(1,j)^(i-1); %Potência de corte
    end

end
%% Escritura do trecho do arquivo input
fid = fopen ('exp07_15um-F4x.txt','wt'); % Abertura do arquivo txt com os trechos para
modificação do input

fprintf (fid, '                    -- HEADER FOR ALL CHIPS: COPY AND PASTE THIS
FRAGMENT IN THE ABAQUS INPUT FILE --\n\n');

fprintf (fid, '\n\n');

% for i=1:n_points-1
%     fprintf (fid,'*Amplitude, name=C1%u-%u, definition=DECAY\n     0.,          %3.3f,
%1.10f,          %1.10f,\n',i,n_points,load(1,i),part_time(1,i),part_time(1,i+1)/3);
```

```matlab
%       fprintf (fid,'*Amplitude, name=C2%u-%u, definition=DECAY\n     0.,          %3.3f,
%1.10f,          %1.10f,\n',i,n_points,load(2,i),part_time(1,i),part_time(1,i+1)/3);
%       fprintf (fid,'*Amplitude, name=C3%u-%u, definition=DECAY\n     0.,          %3.3f,
%1.10f,          %1.10f,\n',i,n_points,load(3,i),part_time(1,i),part_time(1,i+1)/3);
% end

for i=1:n_points % Definição das funções de amplitude de acordo com a quantidade de pontos
em cada cavaco
    if i==1
        fprintf (fid,'*Amplitude, name=C1%u-%u, definition=SMOOTH STEP\n     %1.10f,
%3.3f,     0.0000000005,          0.,\n',i,n_points,part_time(1,i),load(1,i));
        fprintf (fid,'*Amplitude, name=C2%u-%u, definition=SMOOTH STEP\n     %1.10f,
%3.3f,     0.0000000005,          0.,\n',i,n_points,part_time(1,i),load(2,i));
        fprintf (fid,'*Amplitude, name=C3%u-%u, definition=SMOOTH STEP\n     %1.10f,
%3.3f,     0.0000000005,          0.,\n',i,n_points,part_time(1,i),load(3,i));




    elseif i==2
        fprintf (fid,'*Amplitude, name=C1%u-%u, definition=SMOOTH STEP\n     %1.10f,
0.,     0.0000000005,          %3.3f,          %1.10f,          %3.3f,     %1.10f,
0.,\n'...
                                          ,i,n_points,part_time(1,i-1),load(1,i-
1),part_time(1,i),load(1,i),1.1*part_time(1,i));
        fprintf (fid,'*Amplitude, name=C2%u-%u, definition=SMOOTH STEP\n     %1.10f,
0.,     0.0000000005,          %3.3f,          %1.10f,          %3.3f,     %1.10f,
0.,\n'...
                                          ,i,n_points,part_time(1,i-1),load(2,i-
1),part_time(1,i),load(2,i),1.1*part_time(1,i));
        fprintf (fid,'*Amplitude, name=C3%u-%u, definition=SMOOTH STEP\n     %1.10f,
0.,     0.0000000005,          %3.3f,          %1.10f,          %3.3f,     %1.10f,
0.,\n'...
                                          ,i,n_points,part_time(1,i-1),load(3,i-
1),part_time(1,i),load(3,i),1.1*part_time(1,i));
```

```matlab
    else
        fprintf (fid,'*Amplitude, name=C1%u-%u, definition=SMOOTH STEP\n     %1.10f,
0.,      %1.10f,          %3.3f,          %1.10f,          %3.3f,     %1.10f,          0.,\n'...
                                    ,i,n_points,part_time(1,i-
1),1.001*part_time(1,i-1),load(1,i-1),part_time(1,i),load(1,i),1.1*part_time(1,i));
        fprintf (fid,'*Amplitude, name=C2%u-%u, definition=SMOOTH STEP\n     %1.10f,
0.,      %1.10f,          %3.3f,          %1.10f,          %3.3f,     %1.10f,          0.,\n'...
                                    ,i,n_points,part_time(1,i-
1),1.001*part_time(1,i-1),load(2,i-1),part_time(1,i),load(2,i),1.1*part_time(1,i));
        fprintf (fid,'*Amplitude, name=C3%u-%u, definition=SMOOTH STEP\n     %1.10f,
0.,      %1.10f,          %3.3f,          %1.10f,          %3.3f,     %1.10f,          0.,\n'...
                                    ,i,n_points,part_time(1,i-
1),1.001*part_time(1,i-1),load(3,i-1),part_time(1,i),load(3,i),1.1*part_time(1,i));
    end
end

fprintf (fid, '\n\n');

for i=1:n_points % Definição das forças concentradas de acordo com a quantidade de pontos
em cada cavaco
    fprintf(fid,'** Name: CFORCE-%u   Type: Concentrated force\n*Cload, op=NEW,
amplitude=C1%u-%u\nC1-%u, 1, -1\n',3*i-2,i,n_points,i);
    fprintf(fid,'** Name: CFORCE-%u   Type: Concentrated force\n*Cload, op=NEW,
amplitude=C2%u-%u\nC1-%u, 2, 1\n',3*i-1,i,n_points,i);
    fprintf(fid,'** Name: CFORCE-%u   Type: Concentrated force\n*Cflux, op=NEW,
amplitude=C3%u-%u\nC1-%u, 11, 1\n',3*i,i,n_points,i);
end

fprintf (fid, '\n\n');

for i=1:n_chip % Definição das seções com cada material, números dos nós correspondente a
cada cavaco e arquivo de ODB necessário para a simulação
    fprintf (fid, '                    -- CHIP #%u-%u: COPY AND PASTE THIS
FRAGMENT IN THE ABAQUS INPUT FILE --\n\n',i,n_chip);
```

```matlab
    fprintf (fid, '** Section: Section-1-MOD%u\n*Solid Section, elset=MOD%u, material=TI-6AL-4V\n,\n** Section: Section-2-CHIP%u\n*Solid Section, elset=CHIP%u, material=TI-6AL-4V-DEG\n\n\n',i, i, i, i);
    for j=1:n_points
        fprintf (fid, '*Nset, nset=C1-%u, instance=PART-1-1\n%u,\n',j,nodes(i,j));
    end

    fprintf (fid, '\n\n');

    fprintf (fid, '*Initial Conditions, type=STRESS, file=C:/Temp/modelo_50_cavacos_25um/c%u-%u.odb, step=1\n\n\n',i-1,n_chip);
    fprintf (fid, '\n\n\n\n');
end

fclose(fid); % Fechamento do arquivo txt com os trechos para modificação do input
clc

fid = fopen ('simulation.bat','wt'); % Abertura do arquivo txt com os trechos para modificação do input
fprintf (fid, '(\n');
for i=1:n_chip
    fprintf (fid, 'abaqus job=c%u-%u interactive\n',i,n_chip);
end
fprintf (fid, ')');
fclose(fid);

function [picked_node]=analyse_node(node,connected_nodes,a,b,tool_d,i,j,node_chip)

    del_point=zeros(size(connected_nodes,2),2); %Alocação de memória para a variável del_point

    for k=1:size(connected_nodes,2)
        x_node(k,1)=node(connected_nodes(1,k),2);
        y_node(k,1)=node(connected_nodes(1,k),3);
```

```matlab
    del_point(k,1)=connected_nodes(1,k);
    del_point(k,2)=abs((x_node(k,1)-a)^2+(y_node(k,1)-b)^2-((tool_d/2)/1000)^2);
    fprintf('O nó %u tem uma diferença de %3.6f\n',del_point(k,1),del_point(k,2))
 end


plot(x_node,y_node,'ro')


anc_x=node(node_chip(i,j-1),2);
OK=0;


removed_index=0;
while OK~=1
    min_value=1000;
    for aux2=1:size(connected_nodes,2)-removed_index
       for aux3=1:size(connected_nodes,2)-removed_index
          if aux2>=aux3
             continue
          else
             if del_point(aux2,2)<del_point(aux3,2) && del_point(aux2,2)<=min_value
                min_value=del_point(aux2,2);
                picked_node=del_point(aux2,1);
                picked_index=aux2;
             elseif del_point(aux3,2)<del_point(aux2,2) && del_point(aux3,2)<=min_value
                min_value=del_point(aux3,2);
                picked_node=del_point(aux3,1);
                picked_index=aux3;
             else
             end
          end
       end
    end

    picked_x=node(picked_node,2);
```

```matlab
        if picked_x>=anc_x
            del_point(picked_index,:)=[];
            removed_index=removed_index+1;
        else
            OK=1;
        end
    end


    fprintf('Nó selecionado: %u\n\n',picked_node)
        x_picked=node(picked_node,2);
        y_picked=node(picked_node,3);
        plot(x_picked,y_picked,'k+')
end

function [connected_nodes]=connectivity(element,i,j,node_chip)
%Função responsável por encontrar os nós conectados por meio de um elemento
%a um nó particular, sem repetição caso haja.

%Input: i=número do cavaco;j=número do ponto a ser encontrado;node_chip=nó referência
para os outros nós conectados serão encontrados
%Output: connected_nodes = nós conectados ao nó referência

[xp,yp]=find(element==node_chip(i,j-1));

elemet_pos=find(yp==1); % Limpeza dos vetores xp e yp para o encontro do elemento de
número igual ao do nó
xp(elemet_pos,:)=[];
yp(elemet_pos,:)=[];
node_selected=zeros(1,size(yp,1));

    for ind=1:size(node_selected,2)
        switch yp(ind,1)
            case 2
```

```matlab
                node_selected(1,3*ind-2)=element(xp(ind,1),3);
                node_selected(1,3*ind-1)=element(xp(ind,1),4);
                node_selected(1,3*ind)=element(xp(ind,1),5);
            case 3
                node_selected(1,3*ind-2)=element(xp(ind,1),2);
                node_selected(1,3*ind-1)=element(xp(ind,1),4);
                node_selected(1,3*ind)=element(xp(ind,1),5);
            case 4
                node_selected(1,3*ind-2)=element(xp(ind,1),2);
                node_selected(1,3*ind-1)=element(xp(ind,1),3);
                node_selected(1,3*ind)=element(xp(ind,1),5);
            case 5
                node_selected(1,3*ind-2)=element(xp(ind,1),2);
                node_selected(1,3*ind-1)=element(xp(ind,1),3);
                node_selected(1,3*ind)=element(xp(ind,1),4);
            otherwise
        end
    end


index=1;
    for ind=1:size(node_selected,2)


        if ind==1
            connected_nodes(1,index)=node_selected(1,ind);
        else
            pivot=node_selected(1,ind);
            if isempty(find(connected_nodes==pivot))==1
                connected_nodes(1,index)=node_selected(1,ind);
            else
                index=index-1;
            end
        end
        index=index+1;
    end
```

```matlab
    if j<3
    else
        anc_element=find(connected_nodes==node_chip(i,j-2));
        connected_nodes(:,anc_element)=[];
    end

end

function [node_chip]=id_nodev20(tool_d,ae,fz,length,width,n_chip,seed,cutting_angle)
close all

node=xlsread('nos.xlsx');
element=xlsread('elementos.xlsx');

node(:,2)=node(:,2)-min(node(:,2)); %Levará todos os nós para a coordenada X na posição do
vertice inferior esquerdo para a posição (0,0)
node(:,3)=node(:,3)-min(node(:,3)); %Levará todos os nós para a coordenada Y na posição do
vertice inferior esquerdo para a posição (0,0)


%% Encontrar os nós de cada cavacos
theta=(pi/2)-cutting_angle;
%theta_after=(pi/2)-acos(fz/tool_d);
theta_after=0;
initial_number=input('O número do primeiro nó para o primeiro cavaco: ');
initial_ratio=input('Diga em que razão esse número aumenta/diminui: ');

plot(node(1:size(node,1),2),node(1:size(node,1),3),'sg')
axis([0 length/1000 0 width/1000])
hold on

for i=1:n_chip
  a = ((i)*fz)/1000;
```

```matlab
    b = ((tool_d/2)-ae)/1000;
    j=1;


    existing_point=1;
    while existing_point==1
        if j==1
            node_chip(i,j)=initial_number+(i-1)*initial_ratio;
        else


            connected_nodes=connectivityv20(element,i,j,node_chip);
            picked_node=analyse_node(node,connected_nodes,a,b,tool_d,i,j,node_chip);
            ins_theta=theta+(j-2)*(seed/(tool_d/2));


            if ins_theta<=pi/2+theta_after;
                node_chip(i,j)=picked_node;
            else
                existing_point=0;
            end
        end
        j=j+1;
    end
end


end
```

FOLHA DE REGISTRO DO DOCUMENTO

[1.] CLASSIFICAÇÃO/TIPO	[2.] DATA	[3.] REGISTRO N°	[4.] N° DE PÁGINAS
DM	28 de julho de 2016	DCTA/ITA/DM-045/2016	99

[5.] TÍTULO E SUBTÍTULO:

Non conventional method proposal for residual stress simulation generated by end milling process.

[6.] AUTOR(ES):

André Luiz Rocha D' Oliveira

7. INSTITUIÇÃO(ÕES)/ÓRGÃO(S) INTERNO(S)/DIVISÃO(ÕES):

Instituto Tecnológico de Aeronáutica – ITA

[8.] PALAVRAS-CHAVE SUGERIDAS PELO AUTOR:

Milling process, Hybrid method, Numerical modeling, Manufacturing process.

9.PALAVRAS-CHAVE RESULTANTES DE INDEXAÇÃO:

Processos de fabricação; Fresadores; Fresagem (usinagem); Método de elementos finitos; Processos de conformação de metais; Simulação; Tensão residual; Peças mecânica; Engenharia mecânica.

[10.] APRESENTAÇÃO: **X Nacional   Internacional**

ITA, São José dos Campos. Curso de Mestrado. Programa de Pós-Graduação em Engenharia Aeronáutica e Mecânica. Área de Mecânica dos Sólidos e Estruturas. Orientador: Prof. Dr. Alfredo Rocha de Faria. Defesa em 08/07/2016. Publicada em 2016.

[11.] RESUMO:

Surface integrity can be considered as a parameter that is most studied due to its effects on the product performance. The relationship between the functionality and manufacturing variable effects has been mapped, mainly associated with machining process. This process is focused on the connection among the thermo-mechanical loads generated during the process and the residual stresses induced by them. For that reason, industries that have the machining process as the base of the manufacturing chain are naturally interested in these investigations. Additionally, sustainable practices have been put in place, such that for cost reduction, loss reduction and environmental adjustments, optimization of the machining process is demanded. Therefore, validation of functional integrity is more and more required. As experimental procedures are time consuming, alternative computational methods are considered, but only inefficient approaches for complex machining operations are available. Thus, there is need to propose new and efficient one possibility, based on the finite element method, is a hybrid approach for complex machining processes. This approach can be described as the direct application of the machining loads in the workpiece without the necessity of modelling the interaction between tool and workpiece. However, that method was just tested for simple cases of machining, and the application for a more complex process has not been tried yet. Therefore, this work proposes the application of the hybrid method in the end-milling process. This approach resulted in substantial reduction of time for solving the model (from days to hours) with the desired outcomes (residual stress field). The challenges associated with this method were identified as load measurements and the application of these loads, and also the correct definition of the boundary conditions. Another point that was observed is that the residual stress field can be computed without the obligation to apply the loads in the finished shape. That fact renders the machining process easier to model. Finally, even with the simplification of the model, the possibility to expand for other machining processes was confirmed.

[12.] GRAU DE SIGILO:

(X) OSTENSIVO   ( ) RESERVADO   ( ) SECRETO